# UNIVERSITA' DEGLI STUDI DI PADOVA

Sede Amministrativa: Università degli Studi di Padova
Sede Consorziata: Istituto Veneto di Medicina Molecolare

SCUOLA DI DOTTORATO DI RICERCA IN : Bioscienze
INDIRIZZO: Neurobiologia
CICLO: XX

**TITOLO TESI**

# BIOPHYSICAL ANALYSIS OF GAP-JUNCTION CHANNELS INVOLVED IN CONGENITAL DISEASES

**Direttore della Scuola :** Ch.mo Prof. Tullio Pozzan

**Supervisore** :Ch.mo Prof. Fabio Mammano

**Dottorand**o : Victor Hugo Hernandez Gonzalez

31 gennaio 2008

# INDEX

# ABSTRACT

Mutations in connexin genes have been linked to a variety of human diseases, including cardiovascular anomalies, peripheral neuropathies, deafness, skin disorders and cataracts. In connexin-based gap junction channels, each cell contributes a hexamer of connexins forming half a channel, or connexon, which, in the narrow extracellular cleft, interacts with and aligns to another connexon from the adjacent cell. Several endogenous ions and low molecular weight species have been shown to cross gap junction channels, including all current-carrying anions and cations, glycolytic intermediates, vitamins, amino acids, nucleotides, as well as some of the more important second messengers involved in cell signaling, such as InsP3 and cAMP. InsP3 can be considered a global messenger molecule. InsP3 molecules diffuse throughout the cell nearly unbuffered with a diffusion coefficient of 280 $\mu m^2/s$ and lifetime up to 60s in the cytoplasm depending on cell type, interact with specific receptors (InsP3R) present in the endoplasmic reticulum and $Ca^{2+}$ is liberated, raising its concentration in the cytosol. Similar to InsP3, cAMP is a ubiquitous intracellular second messenger that affects cell physiology by directly interacting with effector molecules, including cAMP-dependent protein kinases (PKA), cyclic nucleotide-gated ion channels (CNG channels), hyperpolarization activated channels and the guanine exchange factor EPAC. A variety of specific functions have been proposed for the intercellular transfer of ions and endogenous solutes through gap junction channels, yet the procedures that have gained wide acceptance in assaying the molecular permeability of connexins are dependent on the introduction into living cells of exogenous markers which are then traced in their individual intercellular movements.

Direct measurement of endogenous messengers' transit has been so far problematic mostly due to lack of selective reporters. For example, to compare the transfer rate of cAMP through gap junction channels formed by different connexins, CFTR-mediated chloride currents, $Ca^{2+}$ currents through CNG channels and Ca2+ imaging have been utilized as sensors for cAMP. Defective permeation of cAMP

through gap junctions between adjacent cytoplasmic loops of myelinating Schwann cells has been hypothesized to underlie certain forms of CMTX disease. Also the transfer of InsP3 has been detected indirectly, using $Ca^{2+}$ imaging as the readout for InsP3 dynamics. InsP3 permeability defects detected by a $Ca^{2+}$ reporter system in supporting cells of the auditory sensory epithelium, in which Cx26 and Cx30 are expressed at high levels, have been recently implicated in genetic deafness. In an effort to develop direct, quantitative and reproducible means to monitor the flux of cAMP or InsP3 through recombinant connexin channels, we used novel ratiometric fluorescent biosensors that exploit the phenomenon of FRET for the quantitative monitoring of second messenger concentrations in single living cells in real time. This approach may have a general impact as it provides fast and reliable estimates of connexin permeability to second messengers and permits to investigate their role in the physiology and pathology of cell-cell communication.

# RIASSUNTO DELLA ATTIVITA' SVOLTA

Mutazioni nei geni di connessine sono associate a molte malattie umane, quali anomalie cardiovascolari, neuropatie periferiche, sordità, malattie della pelle e cataratta. Nei canali giunzionali formati da connessine, ciascuna cellula fornisce un esamero di connessine, detto connessone, che forma metà di un canale. Nello spazio intercellulare, questo emi-canale interagisce con a si allinea ad un connessone della membrana della cellula adiacente per formare un poro che mette in comunicazione i due citoplasmi. Molti ioni endogeni e soluti a basso peso molecolare possono attraversare i canali giunzionali. Tra queste molecole si annoverano prodotti della glicolisi, vitamine, aminoacidi, nucleotidi e anche secondi messaggeri, come $InsP_3$ e cAMP. Il primo è considerato un messaggero globale che diffonde facilmente con costante di diffusione pari a 280 $um^2/s$ e con un tempo di vita medio di 60 s nel citoplasma. Interagisce con recettori specifici (InsP3R) presenti nel reticolo endoplasmatico liberando ioni $Ca^{2+}$ nel cytosol. Similmente a $InsP_3$, anche cAMP può essere ritenuto un messaggero globale che influenza la fisiologia cellulare interagendo con PKA, canali CNG, canali attivati da iperpolarizzazione, e fattore EPAC. Il trasferimento intercellulare di ioni e soluti endogeni svolge molte funzioni, eppure le procedure tradizionali utilizzare per saggiare la permeabilità molecolare dei canali giunzionali sono per lo più basate sull'introduzione nelle cellule di marcatori esogeni dei quali si analizza il movimento.

Il monitoraggio diretto del trasferimento di messaggeri endogeni è un problema. Per esempio, il trasferimento di cAMP viene seguito indirettamente, in base agli effetti che produce su correnti cloro in canali CFTR, correnti $Ca^{2+}$ in canali CNG o livelli intracellulari di $Ca^{2+}$. Eppure s'ipotizza che difetti di permeabilità a cAMP siano la causa di talune forme della neuropatia periferica di tipo CMTX. Anche il trasferimento di InsP3 è stato seguito indirettamente, in base agli effetti che produce sui livelli intracellulari di $Ca^{2+}$. Difetti di permeabilità a $InsP_3$ sono stati associati a sordità genetica. Nel tentare di sviluppare un metodo quantitativo, diretto e

riproducibile di monitorare il flusso di cAMP o $InsP_3$, abbiamo utilizzato nuovi biosensori raziometrici fluorescenti che sfruttano il meccanismo di FRET per misurare la concentrazione di secondi messaggeri in tempo reale in cellule vive. La misura contemporanea della conduttanza elettrica giunzionale, ottenuta con la tecnica del doppio patch clamp, combinata con la conoscenza della conduttanza di singolo canale di HCx26, ci ha permesso di stimare il numero di canali attivi in ciascuna placca giunzionale e quindi di stimare la permeabilità unitaria, ossia del singolo canale, a cAMP o $InsP_3$. Per confronto, abbiamo misurato allo stesso modo il flusso di LY. Abbiamo quindi analizzato i risultati in termini di un modello atomico del canale. Questo approccio può avere un impatto generale perché permette di studiare il ruolo svolto dai secondi messaggeri nella fisiopatologia della comunicazione intercellulare.

# Chapter 1

# INTRODUCTION

## 1.1 ANATOMY OF THE INNER EAR

The internal ear or labyrinth, from the complexity of its shape, consists of two parts: the osseous labyrinth, a series of cavities within the petrous part of the temporal bone, and the membranous labyrinth, a series of communicating membranous sacs and ducts, contained within the bony cavities**.** The osseous labyrinth consists of three parts: the vestibule, semicircular canals, and cochlea**.** These are cavities hollowed out of the substance of the bone, and lined by periosteum; they contain a clear fluid, the perilymph, in which the membranous labyrinth is situated (fig. 1-1).

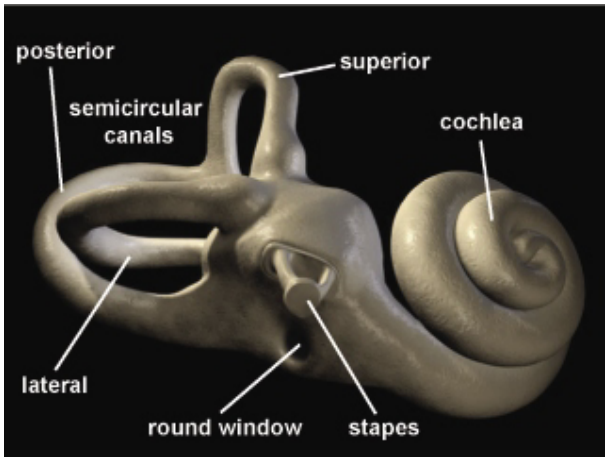


**Figure 1-1. Inner ear.** The inner ear is composed of the vestibular system (*semicircular canals*, utricle, and saccule) and the *cochlea*. Both the *oval window*, where the footplate of the *stapes* inserts, and the *round window* are located at the base of the cochlea.

### 1.1.1 The cochlea

The cochlea bears some resemblance to a common snail-shell; it forms the anterior part of the labyrinth, is conical in form, and placed almost horizontally in front of the vestibule; its apex is directed forward and lateralward, with a slight inclination downward; the base is broad, and appears at the bottom of the internal acoustic meatus. It measures about 5 mm. from base to apex, and its breadth across the base is about 9 mm. The **modiolus** is the conical central axis or pillar of the cochlea. It is perforated by numerous orifices, which transmit filaments of the cochlear division of the acoustic nerve that arrive or come from the **spiral ganglion** (*ganglion of Corti*). The bony canal of the cochlea takes two turns and three-quarters around the modiolus. It is about 30 mm. in length, and diminishes gradually in diameter from the base to the summit, where it terminates in the **cupula,** which forms the apex of the cochlea. The beginning of this canal is about 3 mm. in diameter and presents three openings. One, the **round window,** communicates with the tympanic cavity—in the fresh state this aperture is closed by the **secondary tympanic membrane;** another, of an elliptical form, the oval window, opens into the vestibule. The third is the aperture of the aquaeductus cochleae, leading to a minute funnel-shaped canal, which opens on the inferior surface of the petrous part of the temporal bone and transmits a small vein, and also forms a communication between the subarachnoid cavity and the scala tympani. A delicate lamina, the **osseous spiral lamina,** which projects from the modiolus, reaches about half-way toward the outer wall of the tube, and partially divides its cavity into two passages or scala, of which the upper is named the **scala vestibuli,** while the lower is termed the **scala tympani** which, however, communicate with each other at the apex of the modiolus by a small opening named the **helicotrema**.

The **ductus cochlearis** consists of a spirally arranged tube enclosed in the bony canal of the cochlea and lying along its outer wall. As already stated, the osseous spiral lamina extends only part of the distance between the modiolus and the outer wall of the cochlea, while the **basilar membrane** stretches from its free edge to the

outer wall of the cochlea, and completes the roof of the scala tympani. A second and more delicate membrane, the **vestibular membrane** (*Reissner*) extends from the thickened periosteum covering the osseous spiral lamina to the outer wall of the cochlea, where it is attached at some little distance above the outer edge of the basilar membrane. A canal is thus shut off between the scala tympani below and the scala vestibuli above; this is the **ductus cochlearis** or **scala media**. It is triangular on transverse section, its roof being formed by the vestibular membrane, its outer wall by the periosteum lining the bony canal, and its floor by the membrana basilaris and the outer part of the lamina spiralis ossea. Its extremities are closed; the upper is termed the **lagena** and the lower is lodged in the recessus cochlearis of the vestibule. Near the lower end the scala media is brought into continuity with the saccule by a narrow, short canal, the **canalis reunions**. On the membrana basilaris is situated the **spiral organ** of Corti. The periosteum forming the outer wall of the scala media, is greatly thickened and altered in character, and is called the **spiral ligament**. The upper portion of the spiral ligament contains numerous capillary loops and small bloodvessels, and is termed the **stria vascularis** (fig 1-2).

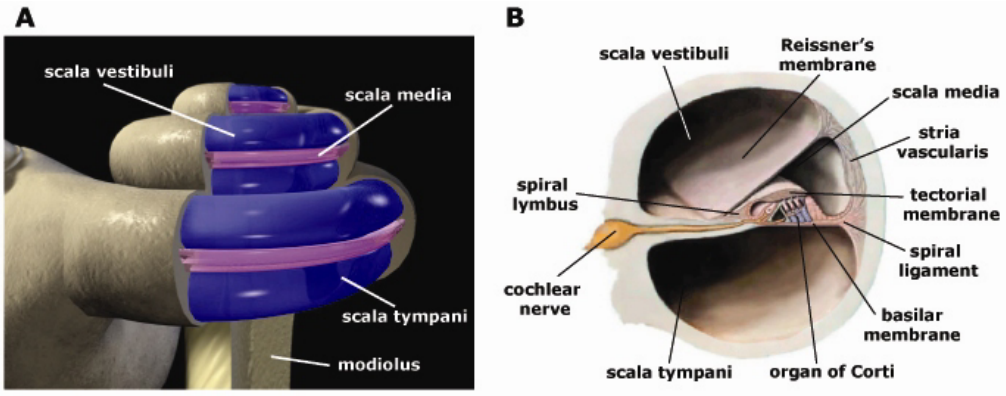


**Figure 1-1 The cochlea.** (**A**) The cochlea is a spiral tube that is coiled around a central pillar, the *modiolus* and is divided into three compartments: *scala vestibuli*, *scala tympani* and *scala media*. (**B**) Cross section through one of the turns of the cochlea. In the spiral canal, the *Reissner's membrane* and *basilar membrane* single out the cochlear duct that separates the scala vestibuli (upper) from the scala tympani (lower). The basilar membrane is stretched between the *lamina spiralis ossea*, on the modiolar side, and the *spiral ligament*, on the outer wall side. The two scalae are filled with *perilymph.* Inside the cochlear duct, the top surface of the *organ of Corti* and the Reissner's membrane isolate a compartment filled with *endolymph*.

### 1.1.2 The spiral organ (of Corti)

The organ of Corti is named after Alfonso Corti, the Italian anatomist who first described it in 1851. Seated on the *basilar membrane* (BM), the spiral organ is an avascular sensory epithelium comprising parallel rows of *sensory hair cells* and several types of *supporting cells*. The basilar membrane together with the overlying organ of Corti and the scala media form the *cochlear duct*. The spiral organ of Corti is covered by the *tectorial membrane*, an acellular gelatinous structure floating in endolymph and originating from the spiral limbus as a thin fibrillar layer that becomes thicker as it extends over the organ of Corti.

The most striking feature of the organ of Corti, when viewed in cross section, is *the tunnel, arch, of Corti* formed by two rows of *pillar cells*. Resting directly on the BM, these cells have adjoining, widely spaced bases that taper upward into slender processes. These, in turn, expand and interlock in the upper surface of the organ of Corti, the *reticular lamina*. The arch separates a single row of pear-shaped, *inner hair cells* (IHCs) from three rows of cylindrical *outer hair cells* (OHCs). IHCs are supported and enclosed by *inner phalangeal cells* whereas each OHC is supported by one *Deiters' cell* that wraps the OHC base in a cup-shaped depression leaving spaces between OHCs. These are approximately 25 μm long in the basal turn and 45 μm long in the apical turn and 6–7 μm in diameter. OHCs are thus suspended by their apical and basal ends within the *space of Nuel* (fig. 1-3).

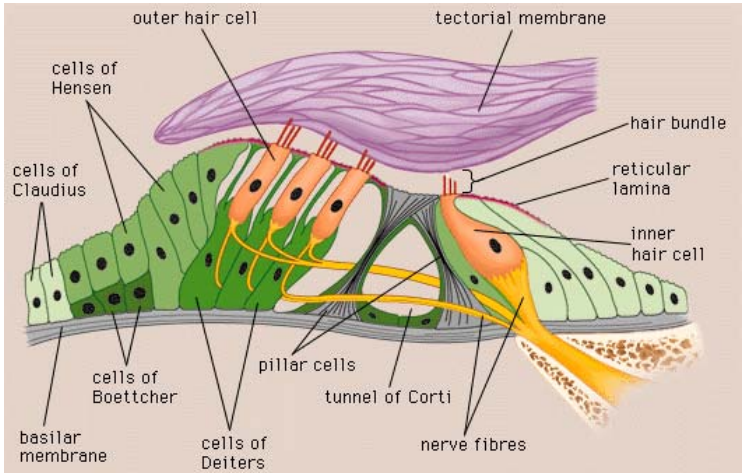


**Figure 1-3. Schematic drawing of a transverse section of the organ of Corti.** Sensory IHCs and OHCs are located on both sides of the tunnel of Corti, limited by the two pillar cells. The tectorial membrane covers the hair cell stereocilia. The IHCs are surrounded by supporting cells while the HCs are firmly "seated" on Deiters's cells. Breaking through the basilar membrane, nerve fibers reach or leave the organ of Corti.

Cochlear hair cells are polarised neuroepithelial cells with primary sensory synapses at their basal end. The characteristic feature of the sensory hair cells is the apical hair bundle, formed by a highly organized array of *stereocilia*, which contains the molecular apparatus devoted to *mechanosensory transduction*. Stereocilia are graded in height, becoming longer on the side away from the modiolus. The tallest stereocilia of the OHCs are firmly embedded in the tectorial membrane, whereas the stereocilia of the inner hair cells are free standing. Stereocilia in a bundle are interlinked by *tip links*, fine extracellular filaments that connect adjacent stereocilia along the *sensitivity axis* [1].

From each Deiters' cell a projection extends upward to the reticular lamina, which is formed by the apposition of the apical poles of pillar cells, OHCs and Deiters' cells. Beyond the OHCs and the Deiters' cells are three other types of epithelial cells, usually called Hensen's, Claudius', and Boettcher's cells. Supporting Hensen's cells are characterized by the presence of abundant lipid inclusions and mitochondria located near their lateral and apical membranes[2]. They posses microvilli

facing the endolymphatic compartment [3], which is a common feature of transporting epithelia [4]. They are adjacent to the outermost row of the OHCs and contact the BM.

### 1.1.3 Endolymph, perilymph and the endocochlear potential

All cell apices forming the reticular lamina are firmly interlocked by *tight junctions*. The tight junction network extends all over the scala media surface of the organ of Corti and into the Reissner's membrane, thus preventing the mixing of endolymph and perilymph. The borders of the endolymphatic space are thus the scala media side of the "upper" surface of the organ of Corti, the stria vascularis and the Reissner's membrane.

Perilymph is similar, but not identical, in composition to other extracellular fluids of the body, such as cerebrospinal fluid: the concentration of $Na^+$ is high, while concentration of $K^+$ is low. It is apparently formed locally from the blood plasma by transport mechanisms that selectively allow substances to cross the walls of the capillaries. However it is unlikely that the cerebrospinal fluid is involved in the normal production of perilymph [5]. A fluid similar to perylimph fills the spaces within the spiral organ (tunnel of Corti and space of Nuel), the **endolymph,** which is unique among extracellular fluids of the body as its $K^+$ concentration is much higher than its $Na^+$ concentration (Table 1). A second striking feature of endolymph is its electrical potential, which is approximately 80 mV more positive than the potential of perilymph (usually taken as reference). This voltage difference is known as the *endocochlear potential* (EP) [6].

**Table 1. Ionic concentrations of perilymph and endolymph (in mM).**

| | Perilymph (scala vestibuli) | Perilymph (scala tympani) | Endolymph (scala media) |
|---|---|---|---|
| $Na^+$ | 141 | 148 | 1.3 |
| $K^+$ | 6.0 | 4.2 | 157 |
| $Ca^{2+}$ | 0.6 | 1.4 | 0.023 |
| $Cl^-$ | 121 | 119 | 132 |
| $HC0_3^-$ | 18 | 21 | 31 |

From Marcus in Cell Physiology *source book* [7].

## 1.2 THE PHYSIOLOGY OF HEARING

### 1.2.1 Overview

Hearing is the process by which the ear transforms acoustic waves into nerve impulses that are conveyed to the brain, where they are interpreted as sound signals. In the process of forming a sound perception in the central nervous system, the incoming acoustic energy undergoes several transformations. Air pressure changes in the external auditory meatus cause the vibrations of the *tympanic membrane* and *middle ear ossicles*. At the end of the ossicular chain, movement of the *stapes* footplate within the oval window of the cochlea, in turn, generates a pressure field within the cochlear fluid, imparting a pressure differential across the BM [8], which in response to sinusoidal pressure applied to the stapes, becomes the site of propagation of so called *travelling waves* [6]. BM motion causes the reticular lamina to slide relative to the tectorial membrane, thus activating the mechanosensory apparatus of the stereocilia, which in turn generates a *receptor potential* in the hair cells. Finally, this promotes

nerve impulse generation in the afferent fibres of the cochlear nerve. Neural activity is transmitted to the brainstem, from which it is relayed, after extensive processing, to the primary auditory area of the cerebral cortex, the ultimate centre of the brain for hearing.

### 1.2.2 Transduction of mechanical vibrations

Hair cell mechanosensory transduction takes advantage of the EP and the high $K^+$ concentration found in endolymph. Deflection of the hair bundle in the excitatory direction (i.e., that of increasing stereocilia length) pulls the tip links and gates directly mechano-sensitive transduction channels in the tips of the stereocilia, admitting $K^+$ into the hair cell [9,10]. *In vitro* measurement from hemi-cochlea preparation, show that, at low frequencies, channels opening occur when the organ of Corti is displaced toward scala vestibuli [11,12]. $K^+$ flow is driven by the large potential difference between endolymph (+80 mV) and hair cell cytoplasm (−70 mV for the OHCs, −45 mV for the IHCs [13]). $K^+$ entry causes depolarization of the cell basolateral membrane (receptor potential) leading to the opening of voltage gated $Ca^{2+}$ channels, $Ca^{2+}$ influx (boosted by CICR) [14-16], release of neurotransmitter (primarily glutamate) from the basal pole of the hair cell[17] and activation of post-synaptic afferent terminals[18-23].

The two classes of sensory cells hosted within the organ of Corti, i.e. the IHCs and the OHCs, perform different functions. IHCs are primarily involved in afferent signalling, whereas receptor potentials in OHCs evoke mechanical responses (electromotility) mediated by a membrane-based molecular motor, named *prestin*, which responds directly to voltage changes across the plasma membrane[24]. Prestin-based electromotility enhances sound-induced vibrations of the BM (a process known as the *cochlear amplifier*[25]), thus endowing the inner ear with its extraordinary sensitivity and frequency selectivity [26]. Wrapping around the OHC basal pole, Deiters' cells also serve to couple mechanically these sensory-motor cells to the basilar

membrane, ensuring efficient force transmission at frequencies above the corner frequency of the membrane RC filter [27,28]. However, this issue is still controversial[29].

### 1.2.3 Frequency mapping

The BM is internally formed by thin elastic fibres tensed across the cochlear duct. The fibres are short and closely packed in the basal region, i.e. close to the stapes, and become longer and sparser proceeding towards the apex of the cochlea, where the BM ends in the helicotrema. Due to the increasing width of the membrane and its decreasing thickness the local stiffness decreases exponentially from the base of the cochlea (i.e. the location of the stapes) to the apex (i.e. the location of the helicotrema). The compound effect of the graded BM stiffness and the variable fluid mass load results in the travelling waves peaking at frequency-dependent locations along the BM (fig.1-4)

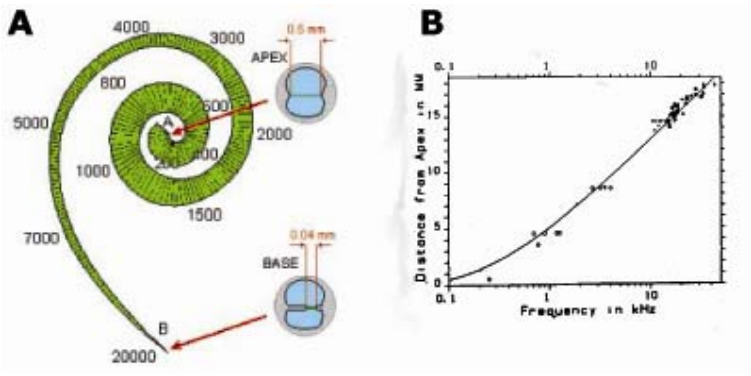


**Figure 1-4.** (**A**) Traveling waves peak at frequency-dependent locations, higher frequencies peaking closer to more basal location. Peak position is an exponential function of input frequency because of the exponentially graded stiffness of the basilar membrane. Part of the stiffness change is due to the increasing width of the membrane and part to its decreasing thickness. (**B**) Relationship between peak frequency (Hz) and distance from apex (nm). From Greenwood *et al.* (1990) [30].

Higher frequencies reach their peak closer to the base whereas tones of lower frequency elicit waves that peak closer to the apex. Peak position is an exponential function of input frequency [30] (tonotopic organization).

## 1.3 $K^+$ HOMEOSTASIS IN THE COCHLEA

### 1.3.1 Endolymph, endocochlear potential and the stria vascularis

In the mouse, a mature ionic composition of endolymph is known to be reached at the end of the first postnatal week. The EP develops 5 to 6 days after birth (P5–P6) and reaches adult values at P17–18[31]. The endolymphatic $K^+$ concentration remains unchanged during the rapid increase of the EP [32]. Thus the EP and the high $K^+$ concentration arise independently during the development of the cochlea. A certain degree of independence had been inferred from the results of anoxia experiments. Anoxia caused a decay to zero of the EP with 1–2 min [33]. Few minutes later, the positive EP was replaced by a negative potential, called –EP, thought to be a diffusion potential arising from the high $K^+$ concentration in the endolymph, which could take several hours to disappear as the ions equilibrated [34].

The current understanding of the molecular processes underlying these phenomena is based on the structure of the stria vascularis, which consists of two barriers formed by the *marginal cells* and the *basal cells*. Each barrier consists of a continuous sheet of cells joined by tight junctions. Between the two layers is the *intrastrial space*, where the potential is +90 to +100 mV relative to perilymph, and a discontinuous layer of *intermediate cells*. Tight junctions are not a simple barrier but they show ion and size selectivity, and the tightness of their barrier function varies significantly depending on cell type. The establishment of the stria vascularis compartment, especially the basal cell barrier, is indispensable for hearing ability through the generation/maintenance of endocochlear potential as it has been shown in claudin KO mice, a cell adhesion molecule working at tight junctions [35] [36].

Gap junctions interconnect basal cells to intermediate cells and to fibrocytes of the spiral ligament, constituting an electrical syncitium. Marginal cells actively remove $K^+$ from the intrastrial space, where $[K^+]$ is kept at 1-2 mM [37].

KCNJ10 (Kir4.1) $K^+$ channels, expressed in the membrane of intermediate cells, provide a route for $K^+$ flow from cytoplasm of the intermediate cells into the

intrastrial space [38]. It is understood that this channel generates the EP in conjunction with a very low [$K^+$] in the intrastrial fluid spaces and a normal (high) [$K^+$] in the cytosol of intermediate cells. Thus, the endocochlear potential is essentially a $K^+$ diffusion potential. Potassium is taken up across the basolateral membrane of strial marginal cells via a $Na^+/2Cl^-/K^+$ cotransporter called SLC12A2 and a $Na^+/K^+$-ATPase. The extrusion of $Na^+$ by $Na^+/K^+$-ATPase establishes a $Na^+$ gradient that energizes the $Na^+/2Cl^-/K^+$ cotransporters for further $K^+$ uptake. $Cl^-$ is removed by basolataral $Cl^-$ channels (CLCK) [39]. KCNQ1/KCNE1 channels (formerly called $I_{SK}$ or min $K^+$ channels) secrete passively $K^+$ from the apical membrane of strial marginal cells. These selective channels activate very slowly (time constant of ~1800 ms) at membrane potentials more positive than –40 mV and deactivate slowly (time constant of 100–400 ms) at membrane potentials more negative than –40 mV [40]. Once activated, the channels do not show any time-dependent inactivation. These properties make these channels ideal carriers of $K^+$ secretion in strial marginal cells since the membrane potential across the apical membrane in these cells is between 0 and +10 mV [41]. Interestingly, the KCNQ1/KCNE1 $K^+$ channel is the sole mechanism that carries $K^+$ secretion across the apical membrane, which makes it an excellent pharmacologic target (Fig. 1-5).

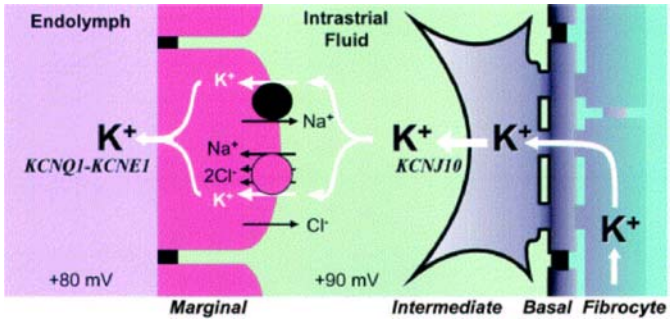


**Figure 1.1 Schematic cross-section through stria vascularis.** Stria vascularis consists of two barriers comprised of cells that are joined by tight junctions. One barrier is comprised of marginal cells and the other of basal cells. Strial marginal cells secrete $K^+$ into endolymph. The endocochlear potential is generated across the basal cell barrier. Basal cells are joined by gap junctions to intermediate cells on the intrastrial side and to fibrocytes on the spiral ligament side. The molecular mechanism that generates the endocochlear potential is understood to be the KCNJ10 $K^+$ channel in the intermediate cells. From Marcus *et al*. (2002) [38].

### 1.3.2 Control of $K^+$ secretion into the endolymph

The critical role $K^+$ plays for endolymph homeostasis and sensory transduction renders it likely that the rate of $K^+$ secretion is controlled by the presence of $K^+$ near the basolateral membrane of strial marginal cells [42] as well as by factors that link the rate of $K^+$ secretion to the systemic status. Strong evidence has been obtained for the presence of purinergic[43] {Housley, 2000 #254}, muscarinic {Wangemann, 2001 #240} and adrenergic receptors {Wangemann, 2002 #161} that act as control mechanisms. $P2Y_2$ subtype of purinergic receptors are expressed on the apical membrane of strial marginal cells, whereas $P2Y_1$ and $P2Y_2$ coexist on the basolateral membrane. The apical $P2Y_2$ receptors down regulate $K^+$ secretion via the DAG-protein kinase (PKC), while basolateral $P2Y_1$ and $P2Y_2$ receptors increase $K^+$ secretion followed by a decline, due to production of $IP_3$ and elevation of cytosolic $Ca^{2+}$ [44]. Although a direct innervation seems not to be present, the lateral cochlear wall has been reported to contain the sympathetic agonist norepinephrine [45], probably derived from blood and stored by melanocytes [45]. The basolateral membrane of strial marginal cells, moreover, contains β1-adrenergic receptors [46] that control the rate of metabolism [47], the activity of $Na^+/K^+$-ATPase [48,49] and the rate of transepithelial $K^+$ secretion [46]. β-adrenergic receptors cause an elevation of the cytosolic cAMP concentration that stimulates KCNQ1/KCNE1 $K^+$ channel in the apical membrane of strial marginal cells to secrete $K^+$ [46,50].

### 1.3.3 Other transport mechanisms contributing to endolymph composition

Sodium is absorbed from endolymph by several cell types, including strial marginal cells, epithelial cells of the spiral prominence, outer sulcus epithelial cells and Reissner's membrane [51]. Epithelial cells in the *outer sulcus* form much of the epithelium between the stria vascularis and the sensory organ. These cells present a

non-selective cation channels in the apical membrane that actively absorbs $Na^+$ which is removed by $Na^+/K^+$-ATPase in the basolateral membrane [51].

Also Reissner's membrane contributes to normal cochlear function by absorption of $Na^+$ from endolymph that enters the cell across the apical membrane through $Na^+$ channels driven by an estimated electrochemical driving force of about +90 Mv {Lee, 2003 #225}. It is removed across the basolateral membrane by $Na^+/K^+$-ATPase and $K^+$, brought into the cell by the pump, subsequently diffuses out through the basolateral $K^+$ channels{Lee, 2003 #225}. Sodium absorption by Reissner's membrane under normal conditions would be expected to contribute only a small negative component to the endocochlear potential.

### 1.3.4 $K^+$ spatial buffering

The steep voltage gradient across the reticular lamina generates a substantial driving force for $K^+$ ions, resulting in a continuous flux of this ion known as the *standing current* [5]. The energy driving current flow is ultimately derived from the activity of the stria vascularis. The standing current flows mostly through the fraction of mechanosensory channels in the sensory cell stereocilia that are open at rest [52]. Potassium is in equilibrium across the basolateral membrane of the hair cell, thus any $K^+$ entering the cell will diffuse out automatically, and will not accumulate inside the cell. In fact, $K^+$ exits the hair cell from the basal pole where $K^+$ channels are found at high density [53]. Thus the cochlear standing current is similar to the retinal dark current in its importance for sensory transduction {Zidanic, 1990 #243}. Based on experiments performed by the end of the '80s, $K^+$ released from the hair cells has been proposed to flow through scala tympani perilymph before to enter the spiral ligament {Johnstone, 1989 #233} {Zidanic, 1990 #243} and to be secreted back into endolymph {Konishi, 1978 #145}{Konishi, 1978 #235} {Salt, 1993 #238} {Sterkers, 1982 #239}. More recently, it has been proposed that both Deiters' and Hensen's cells in the organ of Corti perform a glial-like function, buffering the extracellular

environment and collaborating in the maintenance of cochlear fluids composition [5]. Like the glial syncitium in the central nervous system, all supporting cells in the organ of Corti are massively coupled by *gap junctions* {Tachibana, 1976 #135} {Kikuchi, 1995 #140}{Carmignoto, 2000 #323} {Buniello, 2004 #295} {Forge, 2003 #364}. It has been suggested that $K^+$ released from the hair cells is taken up by adjacent supporting cells and flows from cell to cell via this gap junction system toward the spiral ligament, thereby never entering the perilymph {Spicer, 1996 #248}. This is known as the *potassium recycle hypothesis* [53]. Potasssium exits from OHCs presumably through KCNQ4 $K^+$ channels [54,55] that are exclusively present in the basal membrane [55]. The extremely specialized and tight insertion of the OHC base into the cup region of its supporting Deiters' cell suggests that escape of ions and neurotransmitters from this cellular interface is extremely reduced, if at all possible. Moreover, Deiters' cells are directly reached by nerve terminals which are presumed to be branches of afferent nerve fibres, coming from adjacent OHCs, that may form a local axon reflex carrying information from the sensory cells to the supporting cells through a local circuit [56]. The complexity of this tissue organization suggests that Deiters' cells might play a role in uptake of neurotransmitter and/or $K^+$ from the extracellular fluid [57]. In dual patch clamp recordings from OHC-Deiters' cell pairs *in situ*, depolarizing voltage commands applied to the OHC elicited current deflections of opposite polarities in the OHC (outward $K^+$ current) and the abutting Deiters' cells (inward $K^+$ current) {Lagostena, 2001 #48}. Similar responses have been reported in glial cells of the central nervous system following variations in extracellular $[K^+]$ associated with neuronal cell activation. In the eye, a substantial transfer of $K^+$ from the retina to the vitreous by $K^+$ current flow through Müller cells has been demonstrated after stimulus-related potassium increase [58,59]. The lack of gap junction connections between the two cell types {Forge, 1999 #293} {Lautermann, 1998 #50} and the absence of OHC response following stimulation of Deiters' cells excludes direct electrotonic coupling. Deiters' cells express only low levels of $Na^+/K^+$-ATPase and their membrane conductance is dominated by a $K^+$ channel. Owing to its outward rectification, however, the $K^+$ channel is closed at resting voltages, and hence cannot

mediate $K^+$ uptake. A study of Boettger *et al.* [60] indicates that $K^+$ uptake into Deiters' cells occurs through Kcc4, a $K^+/Cl^-$ cotransporter modulated by protein phosphatase 1 [61]. Unlike active pumping by the $Na^+/K^+$-ATPase, $K^+$ uptake through Kcc4 would be energetically 'cheap' and would occur close to electrochemical equilibrium [60].

According to the $K^+$ recycling hypothesis, $K^+$ cleared from the OHCs move via the supporting cell syncitium through the gap junction systems that provides the basis for long-range electrical and metabolic cell-to-cell communication [62]. The gap junctions would thus provide a route for re-distributing $K^+$ away from regions of activity thereby maintaining hair cell sensitivity [63]. Studies of junctional conductance in isolated Hensen's cells have indicated that the gap junctions are voltage-gated and show rectification {Zhao, 2000 #166}, possibly suggesting a 'one-way flow' consistent with this hypothesis.

Gap junctions are also present between Claudius cells and *root cells*, in the outer sulcus. The root cells extend their cytoplasmic processes into the lower part of the spiral ligament and are connected to fibrocytes, which form gap junctions with the basal cells of the stria vascularis [64] and are also equipped with the $Na^+/2Cl^-/K^+$ cotransporter SLC12A2 [65] and the $Na^+/K^+$-ATPases {McGuirt, 1994 #149}. Recently it has been found the expression of the Kir5.1 subunit in specific types of fibrocytes in the spiral ligament, while Kir4.1 is expressed only in stria vascularis. During development, the expression of Kir5.1 subunits start significantly later than Kir4.1, correlating with the rapid phase of elevation of enocochlear potential. All this could suggest distinct roles of these two Kir channel subunits in the $K^+$ circulation pathway of the cochlea [66]

According to this scheme, the excess $K^+$ entering the Deiters' cells ultimately causes a similar excess of $K^+$ to be released by intermediate cells into the intrastrial space (*spatial buffering*), wherefrom it is taken up by strial marginal cells and secreted back into endolymph, as described above (fig 1-6).

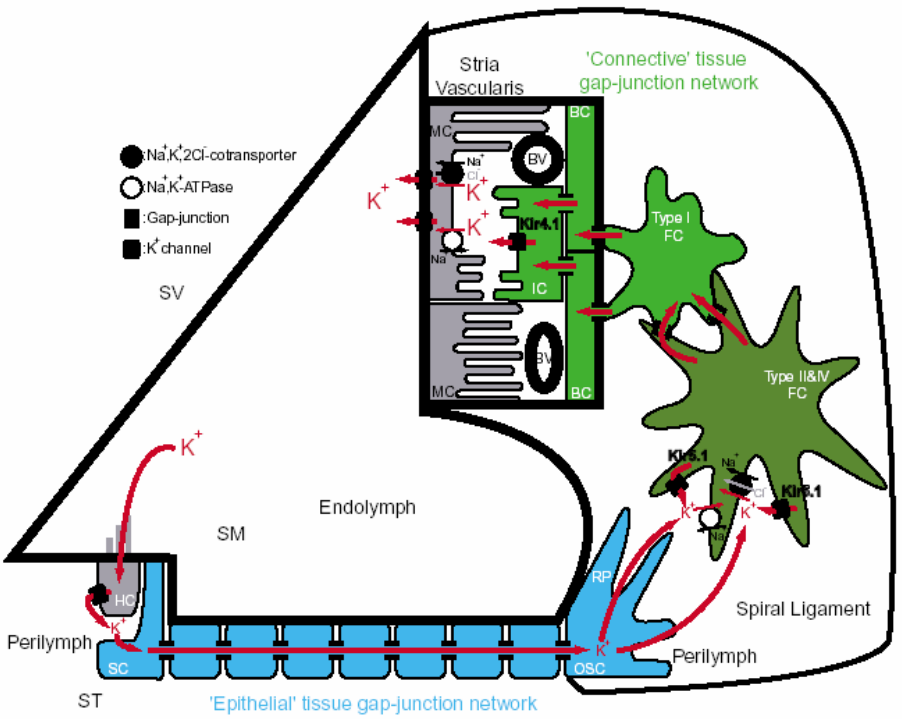


**Figure 1-6. Model of $K^+$ circulation in mammalian cochlea**. $K^+$ exiting from the hair cells is circulated to the spiral ligament through 'epithelial' tissue gap-junction network. $K^+$ is taken up by $Na^+/K^+$ ATPase and $Na^+$, $K^+$, $2Cl^-$ cotransporter expressed in type II and IV fibrocytes, and then recycled to the stria vascularis. Marginal cells (MC) secret $K^+$ to maintain the endolymph. Kir5.1 occurs together with the pump and transporter in the fibrocytes and many adjust their activity for proper amount of $K^+$ transport. Abbreviations: HC, hair cell; SC, supporting cell; OSC, outer sulcus cell; RP, root processes of the OSC; FC, fibrocyte; BC, basal cell; IC, intermediate cell; MC, marginal cell; SV, scala vestibuli; SM, scala media; ST, scala tympani; BV, blood vessels. Blue and green, respectively, indicate the components of 'epithelial' and 'connective' tissue gap-junction networks (from [66])

## 1.4 GAP JUNCTIONS AND CONNEXINS

A gap junction plaque is a zone of close apposition of the membranes of two adjacent cells with a high concentration of up to thousands of gap junction channels [67]. These intercellular channels mediate direct cell-to-cell communication by allowing the passage of ions and molecules as vitamins, small saccarides, aminoacids, nucleotides

and second messengers, up to approximately 1 kDa[68,69]. Gap junction channels play a crucial role in a wide range of physiological processes and are involved in development, cell differentiation, growth and proliferation, electrical activation of the heart and of smooth muscles, neuronal signalling, hormone secretion, sensory transduction, wound healing, lens transparency and immune functions [70]. Abnormal function or expression of connexin genes can generate several diseases including, peripheral neuropathies, cataracts, skin disease or deafness [69]

The structural vision of Cx channels is mainly based on the crystal structure obtained at a resolution of 7.5 Å in the membrane plane of junctional channels formed by Cx43 [71,72]. This 3-D map confirms the presence of 24 transmembrane α-helices within each hemichannel or connexon, corresponding to the four α-helices domains (M1 to M4) of each monomer. The α-helical structure disappears in the extracellular region (i.e., in the ‘‘gap’’), forming a tight electrical and chemical seal to exclude the exchange of substances with the exterior. This continuity of pore wall is consistent with an earlier proposal that the two extracellular loops (E1 and E2) form an antiparallel β-sheet structure stabilized by intramolecular disulfide bonds [73]. The transmembrane α-helical are grouped into two concentric rings around a central pore. One of the two possible helix pairs of a single Cx forms the aqueous pore, while the other helix lines the pore at the cytoplasmic side. The lumen of the channel pore widens to ~ 25 Å at the extracellular side and up to ~ 40Å at the cytoplasmic side. An important limitation of the actual model of the Cx43 channel is that the resolution is still insufficient to permit the assignment of distinct molecular Cx domains. The structure of the peptides corresponding to the NT-domain of rat and human Cx26 [74,75 76], the ‘‘L2’’ sequence of CL-domain and CT-domain of Cx43 [77,78] has been solved by nuclear magnetic resonance (NMR) spectrocopy analysis. These data indicate that the three cytoplasmic domains are likely to be relatively flexible and that small α-helical segments can be found in each (Fig. 1-7). The highest degree of diversity among connexins is found in the CL and the CT, suggesting that many of the functional differences between connexins reside there {Martin, 2004 #13} {Laird, 2006 #461}.

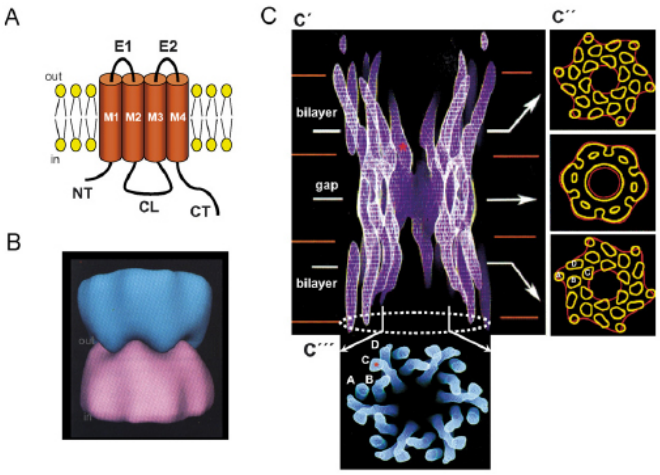


**Figure 1-7. Structure of connexin channel.** (A) All connexins share a tetraspan transmembrane topology (TM1–4) with two extracellular loops (E1, E2) and three intracellular domains: the N- and C-termini (NT, CT) and a cytoplasmic loop (CL) connecting TM2 and TM3. (B). 3D channel structure based on the reconstruction at ~20Å resolution of single Cx32 hemichannels produced by splitting a rat liver junction. The docking model shows the interdigitation between the six-fold connexin subunits of the two apposing hemichannels (in blue and pink). (C). 3D channel structure from 2D crystals of CT truncated Cx43 at 7.5 Å resolution within the plane of membrane bilayer [from Unger et al., 1999]. c' and c'', sagittal-section and cross-sections. Each hemichannel contains 24 transmembrane α-helices packed in a mixed right- and left-handed pattern around the central pore. At the extracellular gap, the α-helical conformation disappears, and a continuous wall isolates the lumen pore from exterior (c'' middle). c''', channel view from cytoplasmic side. The molecular boundary for each subunit was arbitrarily assigned as a 4-helix bundle model in which the α-helices were designed A–D. Accordingly, the B and C pairs line the pore. The C α-helixlines most of the length of the pore and has a kink near outer layer of lipid membrane narrowing the pore to ~15Å (red asterisks in c'). The pore lumen widens to ~25Å toward the extracellular gap and to ~40Å at the cytoplasmic side.

At least 20 distinct human Cx isoforms have been cloned [79] and family members are denominated based on their predicted molecular weight [80]. They have highly conserved sequences and may have originated from a common ancestor [80].

Connexins have a short half-life of only few hours and therefore they must be continually biosynthesized and degraded. Connexins are thought to co-translationally thread in to ER (endoplasmic reticulum), with the possible exception of Cx26 that can be both co- and post- traslationally imported to the ER membranes and even to be directly imported into the plasma membrane {Zhang, 1996 #462} {Ahmad, 2002 #463}. Connexin oligomerization could be a progressive event that begins in the ER and then the stable oligomers are established in the trans-Golgi network [81]. Again,

Cx26 could be the exception since some studies reveal that it can reach the cell surface via a Golgi-independent pathway {George, 1999 #327} {Martin, 2001 #92}. Vesicles transport hemichannels to the plasma membrane shearing the general secretory pathway with other membrane proteins [82]. Once inserted into the plasma membrane, connexons appear to freely diffuse within the membrane to dock with connexons of the adjacent cell to form gap-junction channels [81]. Many tissues express more than one connexin isoform where connexins can form *homomeric* connexons – composed by a single type of connexin – or *heteromeric* connexons – which contain different connexins. Thus *Homotypic* channels are composed of identical connexons, otherwise the channels are *heterotypic* {Kumar, 1996 #326} {Yeager, 2000 #390} (Fig. 1-8). However, not all co-expressed connexins can form heteromeric connexons or heterotypic channels. For example Cx26 can form heteromeric-herotypic channels with Cx30 [83] or Cx32 [84], but is unable to co-oligomerize with Cx43 [85] (table 1). It has been suggested that an ‘‘assembly’’ signal allows connexin subunits to recognize each other, thus preventing the interaction of incompatible connexins [86].

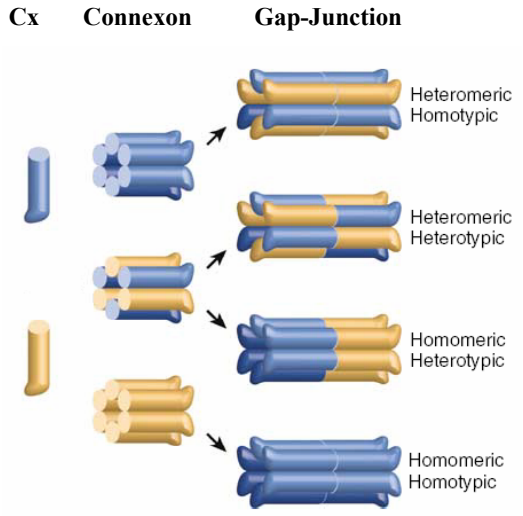


**Figure 1-8.** Six connexins oligomerize to form hemichannels called ‘‘connexons,’’ which then align in the extracellular space to complete the formation of gap junction channels. Different connexins can selectively interact with each other to form homomeric, heteromeric and heterotypic channels, which differ in their content and spatial arrangement of connexin subunits.

| | Cx26 | Cx30 | Cx30.3 | Cx32 | Cx37 | Cx40 | Cx43 | Cx45 | Cx46 | Cx50 |
|---|---|---|---|---|---|---|---|---|---|---|
| Cx50 | + | | | + | | –[b] | –[b] | | + | + |
| Cx46 | + | | | + | | –[b] | + | | + | + |
| Cx45 | –[c] | - | - | –[b,c] | + | + | | + | | |
| Cx43[c] | –[b,c] | - | +[a] | –[b,c] | + | + | + | + | + | +[d] |
| Cx40 | –[b,c] | + | + | –[b,c] | + | + | + | | | |
| Cx37[c] | –[c] | - | +[a] | –[b,c] | + | | + | | | |
| Cx32 | + | +[a] | - | + | | | | | | |
| Cx30.3[c] | | + | + | | | | | | | |
| Cx30 | +[a] | + | | | | | | | | |
| Cx26 | + | + | | + | | | | | | |

**Table 1. Heterotypic and heteromeric compatibility among mammalian Cxs.**

Yellow squares represent HeT Cx compatibility. Green squares represent HeM Cx compatibility. + indicates a compatibility between Cxs, – indicates that the Cxs are incompatible. A blank cell indicates that the relevant experiments determining compatibility have not been performed.

a Unpublished data

b HeT compatibility was assessed in oocyte pairs; therefore, it may not apply in other systems.

c HeT compatibility was assessed with dye coupling; therefore, it may not apply to electrical coupling.

d The chicken homolog of human Cx50 was used (cCx56).

### 1.4.1 Permeability

The number and distribution of gap junction channels is generally relatively stable under physiological conditions. However, the flux of connexins into and out of gap junctions is frequently reported to be highly dynamic [86]. New channels are added to the outside of the junctional plaque while older channels are internalized from the centre to be degraded[86,87]. The regulation of gap junction trafficking, assembly/disassembly and degradation is likely to be critical in the control of intercellular communication and phosphorylation has been implicated in the regulation of the connexin "lifecycle" at several stages[88,89].

Aside their ability to electrically communicate adjacent cells, gap junction channels mediate also intercellular movement of cytoplasmic molecules. Since the first report of functional intercellular molecular signaling [90], several studies have revealed a high degree of selectivity among different connexins. The unitary conductance (i.e. the conductance of a single gap junction channel) varies widely (25

pS for Cx45, 350 pS for Cx37) even though the sequence of monovalent cation selectivity is the same (K>Na>Li>TEA) for different connexins [91]. The charge selectivities range from slightly anion selective (1.1:1 for Cx32 [92]) to highly cation selectivity (10:1 for Cx45 [93]). All these different unitary conductances and charge selectivities suggest that the pores of different connexin channels have diverse properties, structural and/or electrostatic.

Molecular permeability has been classically assessed by the introduction of exogenous tracers into one cell and following its intercellular transfer to the adjacent cells {Weber, 2004 #362}. By employing a wide array of molecular tracers, it has been demonstrated that the selective transfer of molecules through gap junction channels is not dictated by size alone but is affected also by other parameters such as charge or rigidity[91,94]. More recently it has been possible to characterize the permeability of connexin channels to cytoplasmic molecules. Indeed, gap junction channels are permeable to soluble molecules such as cAMP, cGMP, $Ca^{2+}$ and $IP_3$ {Lawrence, 1978 #494} {Saez, 1989 #22} {Sanderson, 1995 #338} {Bevans, 1998 #467} {Bedner, 2006 #470} [95]. It has been shown that permeability to these metabolites depends on several factors. For example, homomeric connexons made of Cx32, expressed in liver parenchymal cells, permitted the transmission of $IP_3$ between cells and the spread of $IP_3$-triggered $Ca^{2+}$ waves {Niessen, 2000 #25}. It has also been shown that Cx32 is permeable to both cAMP and cGMP, whereas heteromeric connexons composed of Cx32 and Cx26 lose permeability to cAMP, but not to cGMP [96] {Niessen, 2000 #25} {Weber, 2004 #362} {Ayad, 2006 #468}. These data suggest that specific high affinity interactions take place between gap junction channels and particular molecules and whose properties cannot be extrapolated in a straightforward way from estimates of pore size, conductance or charge selectivity.

## 1.4.2 Voltage gating

The transfer of ions and other molecules through gap junction channels is regulated by multiple stimuli, including voltage. V*oltage gating* depends both on transjunctional voltage ($V_j$), i.e. the potential difference between the cytoplasm of the two adjacent cells (Fig. 1-9) and on membrane potential ($V_m$).

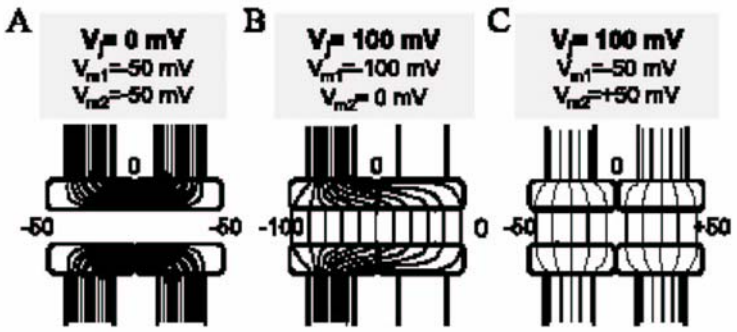


**Figure 1-9** Schematic representation of a GJ channel with presumed isopotential lines when both cells are held at the $V_j$ = 0 mV (**A**), and at $V_j$ = 100 mV (**B** & **C**), but at different values of $V_m$ in each cell. In (**A**) the channel lumen is isopotential with cytoplasms of both cells; $V_{m1}$ = $V_{m2}$ =50 mV. This condition establishes a strong electric field (E) or a high density of isopotential lines across the channel wall in its central region. No $V_j$ is established and E = 0 along the channel pore. GJ channels that respond to this voltage profile are termed $V_m$-sensitive. In (**B**), $V_{m1}$ differs from $V_{m2}$ establishing a $V_j$ and a constant E along the pore; $V_m$ changes along the channel pore from 100 to 0 mV. In (**C**), the same $V_j$ and profile of E along the channel pore are established as in (B), but with different values of $V_{m1}$ (−50 mV) and $V_{m2}$ (50 mV). GJ channels that respond the same way to voltage profiles in (B) and (C) are termed $V_j$-sensitive, but not $V_m$ sensitive. From Bukauskas & Verselis, [97].

In homotypic channels, the junctional conductance, $G_j$ is typically maximal at *Vj=0* ($G_{jmax}$) and it decreases symmetrically for positive and negative *Vj* pulses to non zero conductance values, the residual conductance ($G_{jmin}$) [98]. Junctions with symmetrical bell-shaped steady-state *Gj/Vj* curves and *Gj* transitions of first-order kinetics can be well defined by a single Boltzmann function at each *Vj* polarity, which applies to a two-state system in which the energy difference between states is linearly dependent on voltage. Consequently, in the complete junctional channel there are two mirror symmetrical gates in series, which could act independently or in a contingent manner.

Overall, the recordings at the single-channel level clearly indicate that the Cx channels can contain two distinct *Vj-gating* processes that with different voltage

sensitivity mediate transitions between different conductance states. Some channels exhibit fast $V_j$ gating transitions (~1 ms) to the residual state and slow $V_j$ gate transitions (~10 ms) to the fully closed state [99] , ( Fig. 1-10).

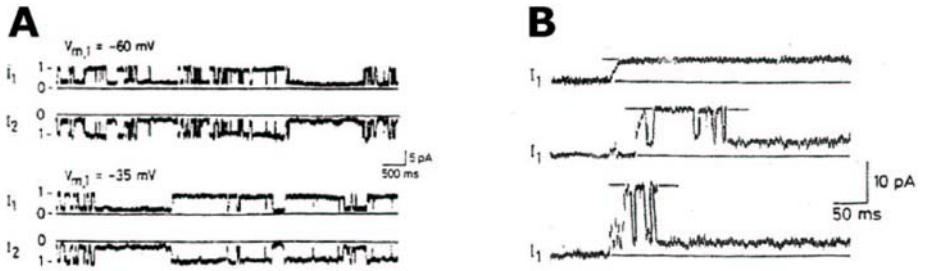


**Figure 1-10. Fast and slow $V_j$ dependence at the single channels level.** (**A**) Examples obtained from insect cell pairs. The transitions to fully open state and to sub-conductance state are fast. (**B**) Example of slow transition to fully open state and fast transition to residual state. From Bukauskas & Weingart (1993)[99].

The NT-domain plays an important role in *Vj* dependence. Studies carried out on Cx32 and Cx26, indicated that the charged amino acid residues in the first positions of the cytoplasmic N-terminal domain, and possibly two positions at the TM1/E1 border, form part of the Vj-gating sensor and of the ionic selectivity filter that determines the Vj-rectifying properties of ion permeation [100-102];[75,103]. The first two residues at the putative TM1/E1 border, also appear to contribute to the initial and steady state *Vj*-dependent processes [100,104,105]. Thus, the valence of the sensor may be determined by the sum of the charges at the NT-domain and at the TM1/E1 border.

Several lines of evidence indicate that the CT-domain is an important component of fast *Vj*-gating. Typically, recordings of macroscopic junctional currents show complex kinetics in response to *Vj* changes with at least a fast component and a slow component. The first evidence indicating that the two kinetic components of *Vj*-

sensitive conductance may be the result of the action of two distinct gating mechanisms was obtained by truncating the CT-domain of hCx32 and rCx43 [106]. Truncation of the CT-domain in both cases ($Cx32_{220stop}$ and $Cx43_{257stop}$) lead to the loss of fast kinetic component and induces novel gating properties largely attributable to the slow gating. In the absence of the CT-domain, junctional currents decay monoexponentially with shorter time constants than those attributed to the slow component in the wt-junctions. According to this, Gonzalez and coworkers [107] conclude that (i) while Cx32wt or Cx43wt hemichannels contain one fast gate and one slow gate, only the slow gate is present in the CT-truncated hemichannels; (ii) both the fast and slow *Vj*-gates seem to close at a negative *Vj* polarity; and (iii) the CT-domain appear to be an integral component of the fast *Vj*-gating mechanism. A simple interpretation of the novel properties of slow gating observed in the absence of fast gate is that the two mechanisms of gating interact electrically in series. Thus, they propose that the classic ball-and-chain model that mediates the fast inactivation in other non related channels could be applicable to the mechanism of fast *Vj* gating in connexin channels. However, recently Peracchia and co-workers have found that the slow gate of Cx32 is active in the absence of uncouplers or mutations and displays unusual *Vj* behavior. They suggest that based on previous evidence for direct calmodulin (CaM) involvement in chemical/slow gating, this may also be CaM-mediated [108].

In some channels, junctional conductance has a double *Vj* and *Vm* sensitivity. The mechanism of *Vm* gating mediates transitions into and out of the fully closed state. Full closure of the channels by *Vm* gating is consistent with the fact that the *Vj* gating properties do not change significantly at different membrane potentials although the macroscopic *Vm* induces large variations in junctional conductance [109]. Mutational analyses carried out in Cx43 have allowed localizing some of the charged residues of the *Vm* sensor in the CT-domain, more proximal to the TM4 than the region for fast *Vj* gating [110]. This *Vm* sensor with a net positive valence would move outwardly to initiate the process of channel closure by depolarizing *Vm*.

### 1.7.3 Chemical gating

Aside of their ability to pass electrical current, gap junctions are also able to mediate intercellular movement of cytoplasmic molecules. Permeability of connexin channels can be altered not only by voltage but also by post-translational modifications. Chemical agents that reduce coupling usually do not leave a residual conductance and their effect is readily reversible (*chemical gating*).

Changes in cell-to-cell communication have been observed after activation of protein kinases [111] [112,113] and protein phosphatases [114] that lead to modifications in tyrosine, serine, and threonine residues [88,89]. Single channel recordings in cells expressing rat Cx43 [115] indicated that under control conditions, three conductive levels could be detected and that the intermediate state was preferred when PKC and PKG kinases were activated. In a similar fashion, phosphorylation of Cx32 by cAMP during PKA activation is correlated with an increase in conductance in hepatocytes [116] [117] or T84 cells [118]. Even though Cx26, one of the connexins present in the supporting cells of the cochlear organ, is not a phosphoprotein [117,119], activation of PKA induce a decrease in permeability to Lucyfer yellow and a reduction in the distribution of unitary conductance [120]. Recently it has been suggested a number of novel post-translational modifications of Cx26 and Cx32, which are likely to be involved in channel trafficking and assembly, or functional modulation [121]. The mechanism by which phosphorylation modifies the unitary conductance of the channels is unknown, but phosphorylation of the connexin carboxyl terminal region is required, and the resulting charge alteration may induce changes in the affinity of the carboxyl-terminus tail to complementary sites located in other intracellular domains, possibly the cytoplasmic loop region, which may modulate the channel to the partially open state.

Both $Ca^{2+}$ and pH play a role in chemical gating of gap junction channels. A long list of evidences have shown that an increase in $[Ca^{2+}]_i$ in a wide range of threshold concentrations, activates the GJ gating mechanism [122]. However, it is clear that this effect is not induced by a direct effect of $Ca^{2+}$ on connexins. This would be

expected to involve clusters of negative charges facing the cytosol. Among connexins, the only conserved acidic residue facing the cytosol is a glutamate that marks the transition between fourth transmembrane (TM4) and CT domains. However, an isolated acidic residue per connexin, even though there would be six of them per connexon, would be incapable of binding $Ca_i^{2+}$ with sufficiently high affinity to account for gating effective $[Ca^{2+}]_i$ in the nanomolar range and would not distinguish between $Ca_i^{2+}$ and $Mg_i^{2+}$; furthermore, this CT region is not believed to be near the pore. Thus, it is reasonable to believe that the $Ca^{2+}$ effect on gating is mediated by an intermediate component. Indeed, recently has been shown that CaM is involved in chemical gating of gap junction channels through a direct interaction with the connexin [123,124] [125], specifically it has been found a CaM-binding sequence comprising residues 136 – 158 in the IC loop of Cx43 [126].

Acidification of internal medium has also been noted to activate connexins gating [122]. The sensitivity to $pH_i$ varies among cell types and connexins [127] and even acts altering in different ways the $V_j$ gating [128]. The data reported so far seem to suggest an indirect effect of $H^+$ on channel gating. It seems that low pH acts through a $Ca^{2+}$ dependent pathway [129] or at least synergistically [130]

Acidification of the cytosol obtained by saturating the perfusion medium with 100% $CO_2$ (as described in the Methods) is often exploited to control the number of active junctional channels in a plaque. When only a few are open, single channel currents can be detected under dual whole cell recording conditions [68].

### 1.4.4 Connexins in the cochlea

Several connexins have been detected in the adult mammalian cochlea {Kikuchi, 1995 #140} {Forge, 2003 #51} {Forge, 2002 #165}[131] {Forge, 2003 #364}. Gap junctions are found in two networks of cells: the *epithelial network* of supporting cells and the *connective tissue network* of fibrocytes and cells of the stria vascularis [83,132]. Cx26 is the most prominent connexin expressed in the inner ear and it is also

expressed in other organs, including the proximal tubules of the kidney, the liver and the rat placenta [80]. The gene which encode for Cx26 is *GJB2,* located in the human chromosome 13q11−12 [80]. Cx26 colocalizes with Cx30 between supporting cells, in the spiral limbus, the spiral ligament and the stria vascularis, where they may form heteromeric connexons {Forge, 2003 #51} {Rabionet, 2000 #44} [133,134]. Cx30 is found also in adult mouse brain and skin [135], is encoded by *GJB6* (which maps to 13q12) and its a.a. sequence shares 77% identity with that of Cx26 [136]. In addition to Cx26 and Cx30, several other connexins are known to be expressed in the inner ear. Cx31 (*GJB3,* 1p32−p36) localize to the inner ear connective tissue. It is expressed at P12 and reaches the adult pattern at P60 {Forge, 2003 #364}. Moreover, measurable mRNA levels for Cx43, Cx37, Cx30.2 and Cx46 have been detected in the stria vascularis [137], although is not clear if these connexins are expressed in the cochlea. Cx43 is expressed in the connective tissues only during development. However, from P8, Cx43 is almost exclusively expressed in the bone of the otic capsule [138].

.

### 1.4.5 Connexins and deafness

According to the data reported by the National Institute on Deafness and Other Communication Disorders (NIDCD) in the United States, hearing loss affects approximately 17 in 1,000 children under age 18 and one of every 1000 infants is born totally deaf. More than half of these cases are caused by genetic factors. Most cases of genetic deafness (70 to 80 percent) are non-syndromic in which there are no additional abnormalities affecting other organs; the remaining cases are caused by specific genetic syndromes.

Non-syndromic deafness presents different patterns of inheritance. Between 75 and 80 percent of cases are inherited in an autosomal recessive pattern (DFNB). Another 20 to 25 percent of non-syndromic deafness cases are autosomal dominant (DFNB). Between 1 and 2 percent of cases show an X-linked pattern of inheritance. Mitochondrial non-syndromic deafness occurs in less than 1 percent of cases.

Many genes are involved in the different types of deafness (syndromic and non-syndromic). It is believed that more than one hundred genes could be involved in hearing impairment. Several of these genes have been identified recently by positional cloning or positional candidate gene approaches [139].

Despite the fact that more than 20 loci have been described for non-syndromic autosomal recessive deafness (DFNB), a single locus, DFNB1, accounts for a high proportion of the cases, with variability depending on the population. The gene involved in this type of deafness is *GJB2* [140-142]. More than 50 distinct recessive mutations of *GJB2* have been described, including nonsense, missense, splicing, frame-shift mutations and in-frame deletions [143]. A large French dominant family affected by pre-lingual deafness showed linkage to chromosome 13q12 (DFNA3), the same region to which DFNB1 had been mapped [144]. An interaction between *GJB2* mutations and a mitochondrial mutation appears to be the cause of hearing impairment in some heterozygote patients {Abe, 2001 #406}. Other connexin genes are also involved in deafness: *GJB1* (Cx32), which is also responsible for X-linked Charcot-Marie-Tooth disease [145]; *GJB3* (Cx31), involved in deafness [146] or a skin disease [147] (erythrokeratodermia variabilis) depending on the location of the mutation; *GJA1* (Cx43), involved in recessive deafness [148]. DFNB1 can also be due to a deletion of 342 Kb involving *GJB6* (Cx30), a gene that is very close to *GJB2* and which has been related to a dominant type of deafness in an Italian family [149,150].

### 1.4.6 Cx26 and autosomal recessive deafness

The most common mutation associated with recessive deafness is a single-base deletion (35delG) within the *GJB2* gene that results in a frame shift at position 12 in the coding sequence of Cx26 and premature termination of the protein [141,151-154]. The precise guanine residue deleted cannot be determined as there are normally six consecutive guanine residues from a.a. positions 30 to 35, and an equivalent mutation has also been described as 30delG in some studies [141,155]. Because this mutation is

common in several ethnic backgrounds, the six repeating guanine residues may represent a "mutational hotspot" within the Cx26 locus, which may explain the prevalence of this mutation in patients with recessive deafness [69].

Besides 35delG, several other Cx26 recessive mutations have been reported {Scott, 1998 #556} {Scott, 1998 #557}. Mutations might affect the correct trafficking and targeting of connexins to the membrane, as demonstrated for the W77R, V37I, S113R, M163V and R184P mutations. Affected proteins, in fact, do not reach the plasma membrane and are retained into intracellular compartments [156]. In other cases, namely V84L and V95M, mutations occur in domains crucial for the control of channel activity and produce a channel with altered functionality, although the proteins appear correctly targeted to the plasma membrane {Bruzzone, 2003 #81} {D'Andrea, 2002 #8} {Wang, 2003 #41}[157].

### 1.4.7 Cx26 and autosomal dominant deafness

One well-characterized example of dominant non-syndromic deafness was attributed to a G-to-C transition that resulted in a tryptophan-to-cysteine substitution at a.a. position 44 (W44C) [158]. Functional analysis of this mutant revealed the inability of W44C mutant channels to allow passage of the fluorescent dye Lucifer Yellow when expressed in HeLa cells [156]. W44C also altered channel activity, when coexpressed with wild-type Cx26 [156]. Additional examples of dominant non-syndromic deafness caused by Cx26 mutations are R143Q, C202F and R75Q. The R143Q mutant affects a highly conserved residue within the third transmembrane domain of Cx26 [159]. The C202F mutation occurs in the fourth transmembrane domain of Cx26 and patients with this mutation exhibited a later onset of hearing loss, with effects becoming evident between 10 and 20 years of age [160]. The R75Q mutation has been analised by our group. R75 in human Cx26 is found at the boundary of the first extracellular loop (E1) and the second transmembrane helix (M2). This mutation produces a non-

syndromic deafness affecting dramatically the function of the channel despite its aggregation in junctional plaques in transfected cells [161].

### 1.4.8 Connexin 30

To date, only a single dominant mutation in *GJB6* has been associated with a rare variant of non-syndromic hearing loss. Replacement of threonine by methionine (T5M) occurs at the amino-terminal end of Cx30 and *in vitro* studies demonstrated the functional impairment of homomeric-homotypic channels formed by the mutant protein, despite normal assembly into gap junctional plaques [150,162]. Rare deletions in *GJB6* have been identified and supposed to cause autosomal recessive DFNA1 [163,164].

### 1.4.9 Connexin 31

Two recessive mutations in *GJB3* have been found to segregate with DFNA1 in Chinese families. These mutations, I141V and I141del, alter the same residue in the third transmembrane domain of Cx31 [146]. Recently, a small in-frame deletion of residue D66 in the first extracellular loop of Cx31 (D66del) has been associated with autosomal dominant non-syndromic hearing loss. Some carriers of this mutation developed also severe neuropathy leading to chronic skin ulcers and osteomyelitis [165]. *In vitro* expression of the mutation D66del demonstrated that gap junction plaques are functionally impaired, resulting in significantly reduced intercellular dye coupling between cells compared to wild-type Cx31 [166].

### 1.4.10 Targeting ablation of inner ear connexins

Gene targeting of connexins in mice has provided new insights into connexin function and the significance of connexin diversity [167]. Complete removal of the Cx26 gene

results in neonatal lethality, thereby preventing analysis of its function in hearing [168]. This limitation was overcome through the generation of a cochlear specific knockout of Cx26 using the Cre–*loxP* system [169], successfully deleting Cx26 in the epithelial gap junction network without effecting Cx26 expression in other organs. Animals with this deletion are a model of recessive deafness and displayed normal patterns of cochlear development, but showed an increase in postnatal cell death within the cochlea along with significant hearing loss. The initiation of cell death was found to occur in IHC's supporting cells, and coincided with the onset of audition. It was hypothesized that loss of Cx26 prevented recycling of $K^+$ after sound stimulation, and that elevated $K^+$ in the extracellular perilymph inhibited uptake of the neurotransmitter glutamate, which accumulated and resulted in cell death [169]. While the evidence concerning Cx26 is compelling, this hypothesis becomes more complex when considering the activity of Cx30 in the inner ear. Lautermann *et al*. [170] have shown that Cx26 and Cx30 normally colocalize within the cochlea, and tissue-specific deletion of the Cx26 gene did not alter expression patterns of Cx30 [169]. This observation complicates the role of gap junctional disfunction in the onset of deafness due to the fact that Cx30 passes $K^+$ in an efficient manner [171] but could not prevent hearing loss in the absence of Cx26. Thus, the presence of a single type of connexin with similar ionic selectivity was unable to rescue the phenotype observed in these mice.

Similar to the tissue-specific loss of Cx26, deletion of Cx30 in mice resulted in hearing loss, but did not alter the development of the inner ear [172]. Although development was normal, Cx30 knockouts lacked the EP, but maintain the $[K^+]$ of the endoplymph. The lack of EP seems to be produced by a disruption of the stria vascularis endothelial barrier due to a significant down-regulation of betaine homocysteine *S*-methyltransferase (*Bhmt*), and resulted in a local increase in homocysteine, a known factor of endothelial dysfunction [173].

In addition, Cx30 knockouts also presented increased apoptosis within the cochlear sensory epithelium. Deletion of Cx30 did not alter the cochlear expression of Cx26, again raising the question of why the continued expression of Cx26 was not

able to compensate for the loss of Cx30 [172]. However, Ahmad and collaborators showed that heterotypic/heteromeric channels are not essential for normal hearing and that the restoration of Cx26 protein level in the cochlea completely rescues hearing in a mouse with $Cx30^{-/-}$ genetic background [174].

One possible explanation for these phenotypes is that gap junctions may have other roles in addition to recycling $K^+$. This idea is supported by data from functional studies showing that, while the $K^+$ conductances of Cx26 and Cx30 are similar, the channels display significant differences regarding the permeability to fluorescent dyes that are similar to cyclic nucleotides and second messengers in both size and charge. These findings indicate that specific loss of either Cx26 or Cx30 within cochlear epithelial cells would not simply reduce the intercellular passage of $K^+$, but would also significantly alter the availability of larger solutes that could be exchanged between the coupled cells [69].

## 1.5 OTHER RELATED PATOLOGIES

### 1.5.1 Connexin and skin disease

In human skin, intercellular communication is mediated by all known β–connexin genes. Autosomal dominant mutations in connexins genes have been linked with several skin disorders which involve an increased thickness of the skin outer layers. This would indicate a critical role for connexins in maintaining the balance between proliferation and differentiation of the epidermis [69,175].

*GJB3* was the first connexin gene reported to cause the autosomal dominant skin disorder erythrokeratodermia variabilis (EKV) and several mutations have been identified so far: G12R, G12D, C86S, R42P and F137L [147].

Dominant mutations in Cx26 have also been described in syndromic deafness associated with skin disease. These disorders include keratitis-ichthyosis-deafness syndrome (KID), palmoplantar keratoderma with deafness (PPK), Vohwinkel syndrome (VS) and hystrix-like ichthyosis-deafness syndrome (HID)

[176,177]. Dominant mutations in *GJB2* affect a.a residues positioned in the highly conserved first extracellular domain (G59A and D66H), or at the boundary of this domain with the first (DelE42) or second (R75W) transmembrane domain. The exact role of Cx26 in skin disease, however, can not be attributed to loss of Cx26 channel activity alone due to the fact that many Cx26 mutations result in non-syndromic deafness. This would indicate that mutant forms of Cx26 associated with skin disorders must impact additional genes in a manner that upsets tissue homeostasis and results in disease.

Different missense mutations in Cx30, G11R, V37E and A88V, affecting conserved a.a. residues positioned in the N–terminal and in the second transmembrane domains, have been identified as cause of ectodermal dysplasia (HED) [178] or Clouston syndrome. These mutations impair trafficking of the protein to the cell membrane and lead to cytoplasmic accumulation when transiently expressed in cultured keratinocytes, thus resulting in a complete loss of gap junction function [162].

### 1.5.2 Connexins and peripheral neuropathy

The first disease associated to mutations in connexin genes was a form of Charcot-Marie-Tooth disease (CMT). Dominant and recessive X-linked mutations in the Cx32 sequence result in progressive degeneration of peripheral nerve and are characterized by distal muscle weakness and atrophy [167,179]. Connexin 32 is present in Schmidt–Lanterman incisures and nodes of Ranvier of myelinating Schwann cells [180,181], providing continuity between the Schwann cell body and the cytoplasmic collar of the myelin sheath adjacent to the axon. It has been suggested that the S26L mutation of Cx32, implicated in X-linked CMTD, alters the permeability of the gap junction to cyclic nucleotides [182]. At least another connexin, possibly Cx31, participates in forming gap junctions in these cells [183]. Connexin 31 was reported to be expressed in mouse auditory and sciatic nerves in a pattern similar to that of mouse Cx32 [165]. The dominant mutation D66del of Cx31, (describe above), is associated with a rare type of

peripheral neuropathy accompanied with mild, often asymmetrical, hearing impairment [165].

## 1.6 FRET Indicators

Chemical sensors for $Ca^{2+}$ or other ions were probably the first to use a change of fluorescence property, such as quantum yield or spectral profile. Nowadays, a broad spectra of molecular physiological indicators, often based on GFP, are available for measuring $H^+$ concentration [184,185], $Zn^{2+}$ concentration[186], $Cl^-$ concentration[187] and $Ca^{2+}$ concentration[188-191]. In addition, biologically active sequences can be incorporated into the fluorescent probe and targeted to specific cellular compartments.

A particular class of compound sensors is based on a change in the efficiency of Fluorescence (also called Förster) Resonance Energy Transfer **(FRET)** between a donor and acceptor GFP variant fused to protein domains or subunits that change their interaction upon ligand binding (fig. 1-11).

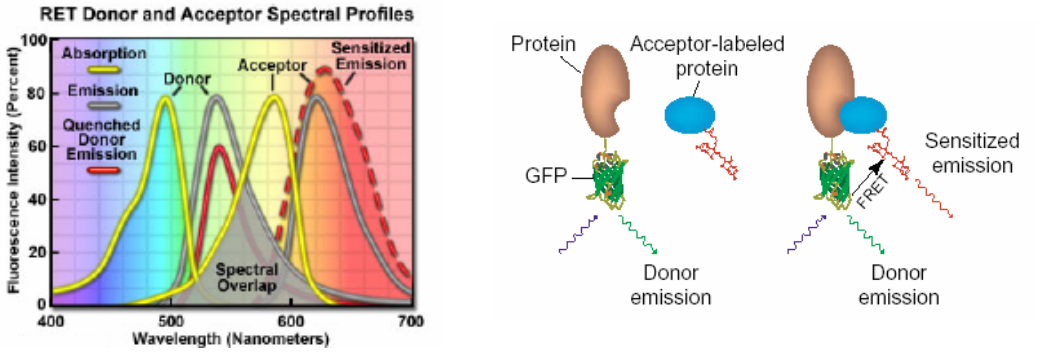


**Figure. 1-11. FRET fenomena.** Overlap (gray area) between the donor emission (central gray curve) and acceptor absorption spectra (central yellow curve) is required for the process to occur. When this overlap is present, and the donor and acceptor are separated by less than 10 nanometers, donor excitation energy can be transferred non- radiatively to the acceptor. The net result is quenching of the donor fluorescence emission (red curve) and an increase in the emission intensity of the acceptor (sensitized emission, red dashed curve). In molecular FRET probes (on the right) a conformational change occurs following binding of a specific ligand, thus modifying the structure of the molecule and changing the distance between the fluorophores. Changes on FRET efficiency between the CFP and YFP tags allow detection of this conformational change.

Interactions between two proteins can be imaged by detecting FRET between donor and acceptor fluorophores. FRET is a photophysical phenomenon where energy is transferred non-radiatively from a donor fluorophore to an acceptor fluorophore with an efficiency defined by:

$$E = \frac{R_0^6}{R_0^6 + r^6}$$

where $r$ is the distance between the two fluorophores, and $R_0$ is the distance at which 50% energy transfer takes place (typically 2–6 nm). The efficiency of resonance energy transfer varies with the degree of spectral overlap, but most importantly *as the inverse of the sixth power of the distance* (radius, $r$) separating the donor and acceptor chromophores. Energy transfer to the acceptor requires the distance between the chromophores to be relatively close, within the limiting boundaries of 1 to 10 nanometers (Förster radius).

There are a number of ways to measure FRET in a microscope that can be broadly divided into intensity-based methods and fluorescence decay-kinetics-based methods with different strategies for its analysis[192-194]. Excitation of a donor fluorophore in a FRET pair leads to quenching of donor emission and in an increased, sensitized, acceptor emission. Intensity-based FRET detection techniques make use of these effects.

FRET has become an important tool for the analysis of interactions among biological macromolecules and for biological sensor applications [95,189,190,195].

## 1.7 AIM AND SIGNIFICANCE OF THIS WORK

Several endogenous low-molecular-weight species cross gap junction channels, including all current-carrying anions and cations, glycolytic intermediates, vitamins, amino acids and nucleotides, as well as some of the more important second messengers involved in cell signaling, such as InsP3 and cAMP[91].

The procedures that have gained wide acceptance in assaying the molecular permeability of connexins, however, are dependent on the introduction into living cells of exogenous markers, which are then traced in their individual intercellular movements [91]. A more commonly used dye is LY (molecular weight, 443 Da; charge, –2), whose high fluorescence efficiency ensures its detection at minute levels. Studies based on LY and other charged tracers, such as the Alexa series of fluorescent probes, show clearly that the permeability profile of each connexin channel is distinct [91]. As even modest selectivity at cellular junctions could have a great effect on the strength, character and location of the transmitted signal, the mechanisms of such discrimination are of acute biological and medical interest [68]. For instance, defective permeation of cAMP through gap junctions between adjacent cytoplasmic loops of myelinating Schwann cells is thought to underlie certain forms of X-linked Charcot-Marie-Tooth disease[182]. However, extrapolations from dye permeation studies present major difficulties because of the different shapes, flexibilities, charges and charge distributions of these molecules [68]. Thus, how exactly these measurements relate to the selective permeability of endogenous solutes remains obscure.

Measurement of endogenous messengers' transit has been so far problematic mostly owing to lack of direct reporters. For example, to compare the transfer rate of cAMP through gap junction channels formed by different connexins, CFTRmediated chloride currents[196], $Ca^{2+}$ currents through CNG channels and $Ca^{2+}$ imaging[197] are used as sensors for cAMP. The transfer of InsP3 also is usually detected indirectly [198].

Using $Ca^{2+}$ imaging as the readout for InsP3 dynamics, our group demonstrated that InsP3 permeability is altered in a deafness mutant of Cx26 [157] .

In the present thesis job, I present the results aimed to determine both the electric and metabolic permeability of gap junction channels using novel ratiometric fluorescent biosensors that exploit the phenomenon of FRET for the quantitative monitoring of second-messenger concentrations in single living cells in real time[195,199]. Wild-type and mutant connexins were expressed into a HeLa cell line devoid of gap junctions[94] from cDNA of human origin. Experiments were performed on a high performance optical recording system available in our laboratory using image acquisition and processing software developed by our group[200,201].

Measurement of junctional conductance, $g_j$, by the dual whole-cell patch-clamp technique, combined with knowledge of the unitary conductance, $g$, of homotypic channels formed by HCx26wt, allowed estimation of the number of active gap junction channels, thus determining the unitary — that is, single-pore — permeability coefficient, $p_u$, for InsP3 and cAMP. The flux of LY was quantified similarly, for comparison. This approach may have general applicability, as it provides fast and reliable estimates of connexin channel permeability to second messengers and permits the study of their role in the physiology and pathology of cell-cell communication. This method permits quantification of defects of metabolic coupling and can be used to investigate interdependence of intercellular diffusion and cross-talk between diverse signaling pathways.

# Chapter 2

# METHODS

The detailed protocols employed during this work are described in the annexed articles. A brief description of these methods is presented here.

## 2.1 Cell culture and transfection

A clone of HeLa cells essentially devoid of connexins [94] (provided by K. Willecke; University of Bonn, Germany) and cultured according to standard procedures. For intracellular delivery of InsP3 and cAMP (see below), we cotransfected cells with the pcDNA3.1 expression vector carrying the coding region of (untagged) HCx26wt (Roberto Bruzzone; Institute Pasteur, China) and an additional expression vector carrying either the InsP3 reporter LIBRA[199] (A. Tanimura; Health Sciences University of Hokkaido, Japan) or the cAMP reporter CFP–Epac(dDEP-CD)–YFP16 (here called H30 for brevity; K. Jalink; The Netherlands cancer Institute) with the Lipofectamine transfection protocol (Gibco, Invitrogen, Leek, The Netherlands) 24 h after plating and experiments were performed 24 h after transfection.

## 2.2. Electrophysiology

For electrophysiological recordings cells were grown on thin (No. 0) coverslips and transfected with HCx26wt. Cultures were then transferred to an experimental chamber

mounted on the stage of an upright wide-field fluorescence microscope (BX51, Olympus Optical Corporation) equipped with an infinity-corrected water immersion objective (60X, 0.90 NA, LUMPlanFl, Olympus) and continuously superfused at 2 ml/min in a standard extracellular solution (ECS), which contained in mM, 150 NaCl, 5 KCl, 1 $MgCl_2$, 10 HEPES, 2 $CaCl_2$, 2 pyruvate and 5 glucose (pH 7.4). Patch pipettes were filled with an intracellular solution (ICS) containing in mM, 120 potassium aspartate, 10 TEA chloride, 1 $MgCl_2$, 10 HEPES, 10 CsCl, 0.3 GTP-Na and 3 ATP-K (adjusted to pH 7.2 with KOH), and filtered through 0.22-mm pores (Millipore). Pipette resistances were 3–5 MΩ when immersed in the bath.

To measure junctional conductance, each cell of a pair was voltage clamped independently with one of the two List EPC-7 amplifiers and kept the two at the same holding potential, *Φ*h. By stepping the voltage in cell 1 while keeping the potential of cell 2 at *Φ*h, thus establishing a 15-mV transient transjunctional voltage $\Phi_j \equiv \Phi_1 - \Phi_2 = \Delta\Phi_1$, we measured junctional current, $I_j$, directly as a change in current in the unstepped cell ($I_j = -\Delta I_2$) (fig.2-1)

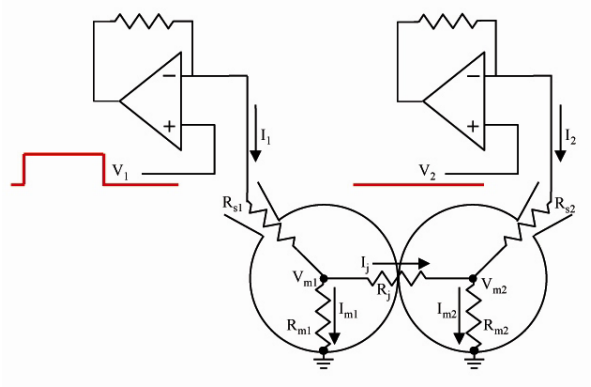


**Figure 2-1. Dual whole cell recording configuration.** Equivalent resistive circuit for the whole cell patch clamp recording configuration from two coupled cells (drawn as tangent circles). $I_1$ and $I_2$, whole cell currents; $V_1$ and $V_2$, command potential applied via each patch clamp amplifier; $V_{m1}$ and $V_{m2}$, cell membrane potential; $R_{s1}$ and $R_{s2}$, series resistance; $R_{m1}$ and $R_{m2}$, cell input resistance; $R_j$, junctional resistance. Accurate junctional current signals are achieved when a majority of the current in response to a transjunctional voltage difference ($V_j$ = $V_{m1}$ — $V_{m2}$) flows across the junction (horizontal arrow) instead of the cell membrane.

## 2.3 Intracellular delivery of permeant molecules

For molecular transfer assays, LY was dissolved in ICS at a concentration of 440 mM. We added cAMP (120 mM, Sigma-Aldrich) to ICS together with IBMX (100 mM, Sigma-Aldrich), a phosphodiesterase inhibitor; dideoxyadenosine (1 mM, Calbiochem), a non-competitive adenylate cyclase inhibitor; and thapsigargin (1 mM, Sigma- Aldrich), a blocker of the SERCA pumps. We added InsP3 (5 mM, Calbiochem) to ICS together with diphosphoglyceric acid (3.5 mM, Sigma-Aldrich), a competitive inhibitor of InsP3 phosphomonoesterases[202] that convert InsP3 into InsP2; and InsP3- kinase inhibitor (20 mM, Calbiochem), a competitive inhibitor of the InsP3 kinase that catalyzes the conversion of InsP3 to InsP4. All solutions were adjusted to pH 7.2 with KOH and filtered through 0.22-mm pores.

For InsP3, we obtained recordings from cells superfused in ECS supplemented with 200 mM suramin, a broad-spectrum P2Y receptor antagonist, to inhibit paracrine amplification of InsP3 signals. In all permeability assays, both cells were approached by pipettes containing identical intracellular solutions and maintained in the cell-attach configuration. A few seconds after the onset of the recording, we ruptured the patch of membrane under the pipette sealed to cell 1 while leaving the seal intact (whole-cell recording conditions for cell 1, WC1), allowing the compound of interest to fill the cell by passive diffusion from the patch pipette. By the end of the recording interval, we also established whole-cell recording conditions for cell 2 (WC2), which permitted an assay of its reaction to direct delivery of the compound and measurement of $g_j$ in response to scaled FVAL pulses. We then applied $CO_2$ to prove that transfer occurred through gap junction channels. Only cell pairs that showed complete uncoupling by the $CO_2$ were retained for the analysis. With LY in the patch pipettes, $g_j$ was constant over this time span; we therefore estimated the number of open channels $N_{pore} = g_j / \gamma$ in the interval between the WC1 and WC2 events from the average of $g_j$ in a 1-min interval after the WC2 event (excluding transients owing to incomplete seal openings). In contrast, similar control

experiments revealed a progressive decline of $g_j$ that was more pronounced for cAMP (average rate of loss 0.37 ± 0.04 nS/s, n = 10) than for InsP3 (0.07 ± 0.03 nS/s, n = 8). Therefore, $g_j$ values collected in a 1-min interval after the WC2 event (excluding transients) were used to extrapolate back to the WC1–WC2 interval.

# Chapter 3

# RESULTS

Part of the results obtained during this thesis work has been published in the articles annexed to this report. Here I only report the results that are not present in the cited papers.

## 3.1 Junctional-Conductance analysis of Cx32 functional mutations involved in X-linked Charcot-Marie-Tooth disease

Charcot–Marie–Tooth disease (CMTX) is a heterogeneous inherited neuropathy characterized by loss of muscle tissue and touch sensation, predominantly in the feet and legs but also in the hands and arms in the advanced stages of disease. Though presently incurable, this disease is one of the most common inherited neurological disorders. The X-linked form of this syndrome is caused by mutations in connexin32 (Cx32), expressed by Schwann cells where it forms reflexive channels that allow the passage of ions and signaling molecules across the myelin sheath. Although most mutations result in loss of function, several studies have reported that some retain the ability to form homotypic intercellular channels but display gating abnormalities, the so-called functional mutations, which retain the basic capacity to ensure electrical coupling but display gating abnormalities[182,203,204]. Since one of the distinctive properties of connexin channels is the ability to allow the passage of molecules up to a certain molecular mass (usually below 1 kDa), it has been postulated that these functional mutations may also exhibit altered size cutoffs[182,203]. Nevertheless, only

limited information is available thus far, and the S26L variant remains the only example in which a substantial reduction in pore radius of the channel open state has been demonstrated for a CMTX associated or any connexin mutation[182].

To gain insight into the molecular defect of three functional CMTX variants, S26L, Δ111 – 116 and R220stop, I have analyzed their biophysical properties respect to those of wild-type Cx32.

Employing dual patch clamp recordings junctional conductance was estimated between cell pairs transfected with the different constructs. The levels of macroscopic conductance of doublets expressing either HCx32wt (21.82 ± 3.3 pS) or R220stop (19.15 ± 4.51 pS) were found to be similar, whereas the percentage of coupled pairs was variable in the case of S26L and Δ111–116, with a very low junctional conductance however (fig. 3-1).

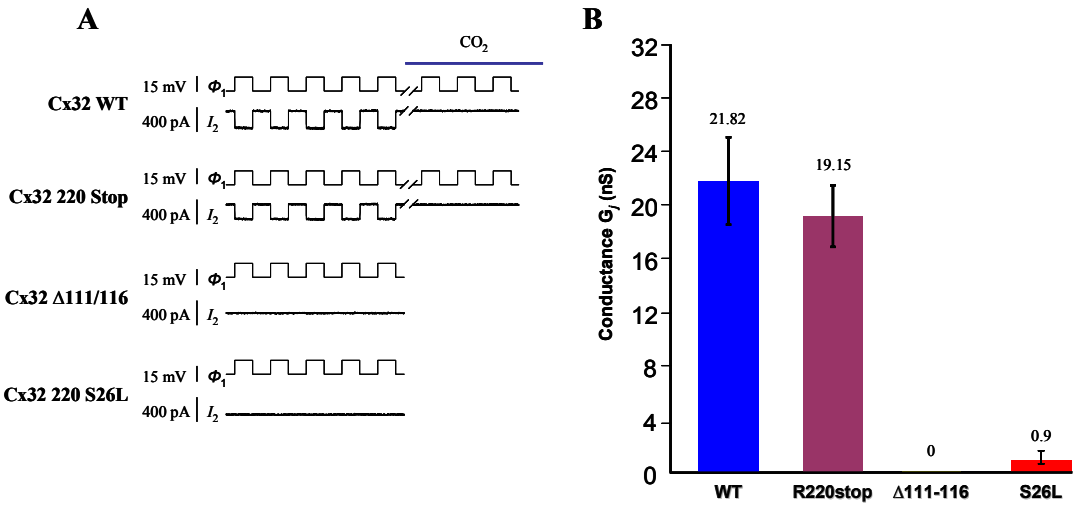


**Figure 3-1.** Junctional conductance and coupling indexes of three Cx32 CMTX mutations. (A) and (B) Voltage and current traces showing that the mutants have a reduced G*j* compared with that of the CX32 WT. To block gap junction channels cells were superfused with a solution saturated with $CO_2$, the transjunctional current disappears, showing thus that the cells are indeed communicated by gap junctions.

## 3.2 Junctional-Conductance analysis of molecular modified mutants causing genetic diseases

Based on a model of canonical α-helices corresponding to the M1–M4 segments, which specifies the approximate positions of α-carbons in the TM domain, [205] we have analysed the electrophysiologycal consecuences of aminoacid substitutions in mutant connexins involved in CMTX diseases and genetic deafness.

Connexin trafficking to and insertion into the plasma membrane is dependent on several factors and processes as the proper folding and oligomerization of the protein [206]; substantial disruption of the protein stability could therefore result in mislocalized protein. The Cα-model of connexins permits to predict which residues are located in proximity to one another and can serve as a basis on which to formulate explicit hypotheses on interactions between amino acid positions. Fleishman and collaborators [207] introduced single and double mutations into the connexin TM domain. A destabilizing mutation would show connexin TM domain aberrant localization outside the plasma membrane. However, a chosen second-site mutation could stabilize the mutated protein and retrieve the wild-type localization at the sites of cell-cell apposition.

In collaboration with the group of Prof. Karen Avraham (University of Tel-Aviv, Israel), we have analysed the electrophysiologycal properties of two deafness causing mutants, Cx26-S139N which is found in the cytoplasm of the cells but not in the plasma membrane, and Cx26-N206S that shows a normal localization in the cells[208,209]. When this pair is doubly mutated, one disease-causing mutation (N206S) compensates for the effects of the other, restoring wild-type localization (fig 3-2). In the same way, the Cx32-R32E is not found in the membrane of adjacent cells, the double mutant Cx32R32E/E142R rescues this mislocalization (fig 3-2). Thus it was interesting to analyse the permeability properties of these mutants to know if the rescue in the mislocalization was able to form functional channels.

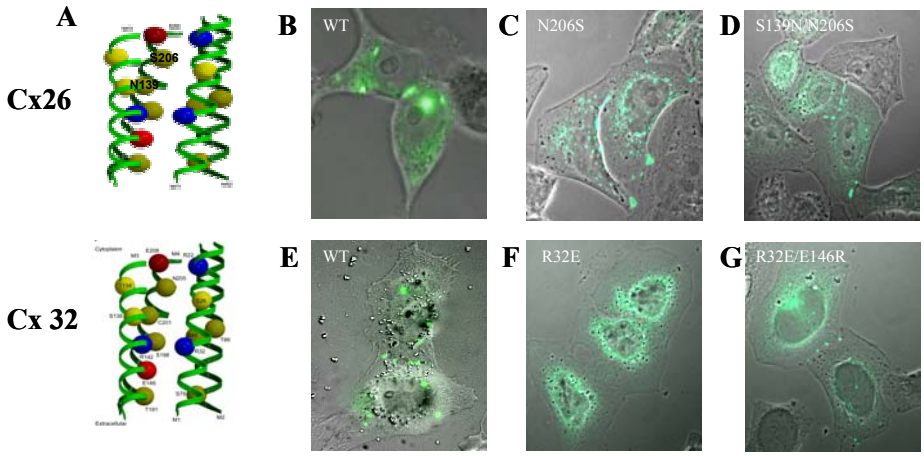


**Figure 3-2. Pattern expression mutant connexins transfected in HeLa cells.** (A) Molecular model of the two connexins, 26 and 32 respectively, where it is showed the residues mutated. (B) Localization in the cell of Cx26 WT. This connexin forms well defined plaques in the contacted membranes. (C) The Cx26-N206S mutant also goes to the membrane and form plaques. (D) The compensatory mutation for Cx26-S138N, S138N/N206S also presents a phenotype of plaques. (E) Cx 32WT, is organized in dots in the membrane of the contacted cells. (F) Cx32-R32E mutant is impaired in its intracellular trafficking and fails to reach the plasma membrane; the compensatory mutation R32E/E146R (G) brings the protein to the membrane similar to that found in the WT (mutant images from [207]).

We transfected HeLa cells with the double mutant constructs and corroborated the normal localization of these mutant connexins in the contact membranes of adjacent cells. Employing dual patch clamp recordings, we estimated junctional conductance between cell pairs. The single Cx26 deafness causing mutant N206S retain a very low junctional conductance of 2.36 ± 0.9 nS (n= 13). The levels of macroscopic conductance of doublets expressing either Cx26-N206S/S139 (n=20) or Cx32-R32E/E146R were 0.14 ± 0.06 nS and 0 nS (n=6), respectively (fig. 3-3).

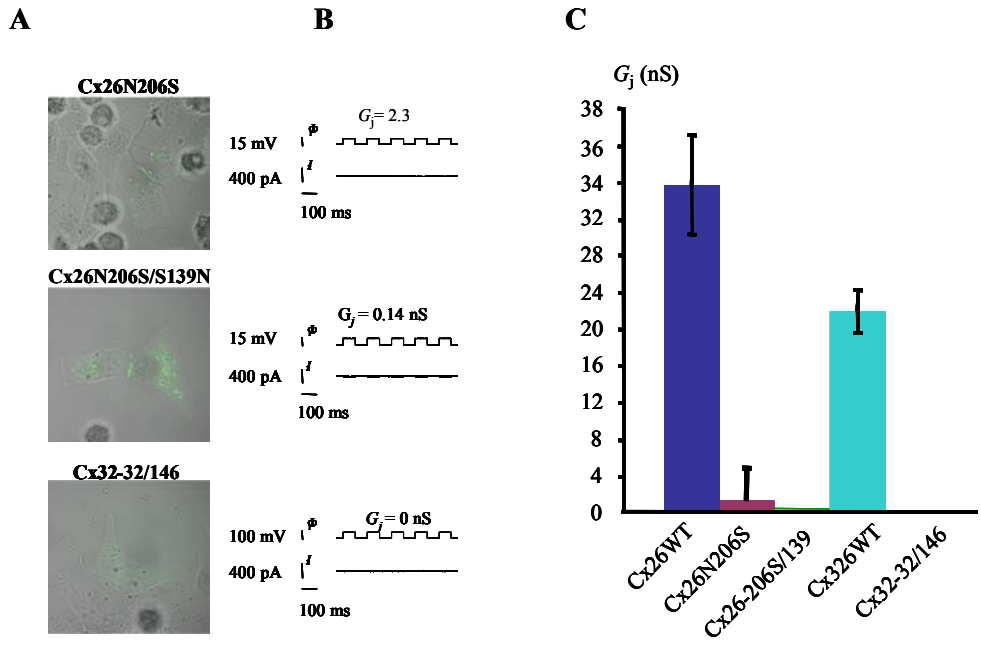


**Figure 3-3.** Junctional conductance of the Cx26 and Cx32 mutants. (A) DIC images merged with fluorescence patterns of three different mutants, for Cx26 and Cx32. (B) Voltage and current traces obtained after achieving the whole cell configuration permit to measure junctional conductance $Gj = -\Delta I_2/\Delta\Phi_1$ As it is shown in (C) all the mutants tested have a reduced G*j* compared with the wild type.

## 3.3 Junctional-Conductance analysis of the new Cx26-L56V mutation

In collaboration with Dr. Annamaria Franze (Istituto di Genetica e Biofisica 'A. Buzzati-Traverso', Naples, Italy) I have also analysed a new Cx26 mutation. Her research group isolated the Cx26-L56V mutation from an Italian family. This mutation is presented in cis-conformation associated with the M34T mutation that has been analysed previously by our group [210]. For this reason it was important to

determine the conductance characteristics of the L56V mutant, either isolated or in its native form associated with the M34T mutation.

When Cx26-L56V is tranfected into HeLa cells it forms plaques in the contact zone of adjacent membranes. Analysing the conductance behavior of this mutant I found that it presents a $G_j$ very similar to that found in the WTCx, and that it is blocked after the acidification of the internal medium. However, when this mutation is associated with the M34T, the $G_j$ is blocked completely (fig.3-4).

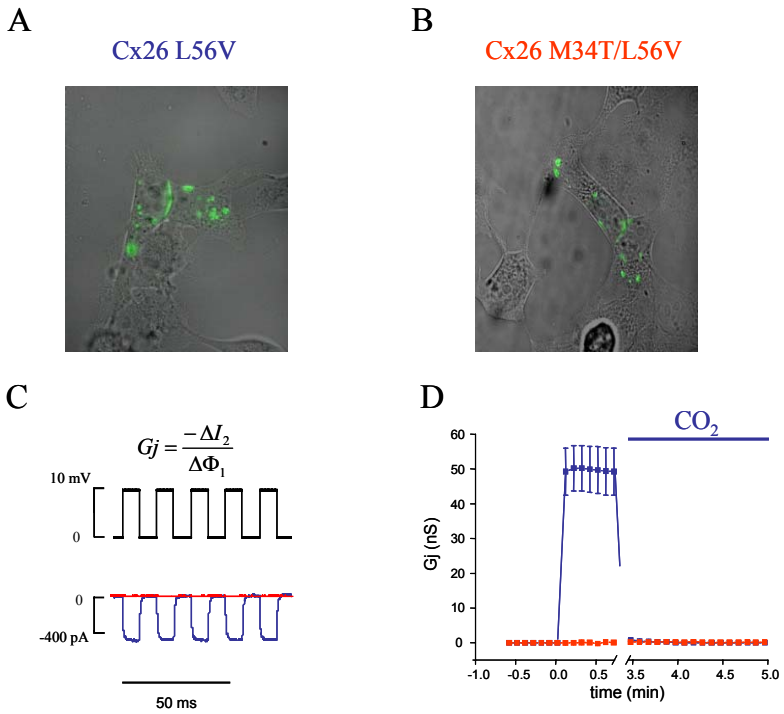


**Figure 3-4. Gj conductance of the new Cx26 mutant L56V/M34T.** (A and B) Merge micrographs of DIC and fluorescent pattern of Cx26-L56V and M34T/L56V, respectively. In both cases the localization of the protein is normal. (C) Junctional conductance of both mutants. Cx26 L56V (blue traces), has a very similar conductance to the WT channel, including its closure after perfusion with an EC solution saturated in $CO_2$, however in its native form, associated with the mutation M34T, it loses all the electrical properties (red traces) (C and D).

# Chapter 4

# DISCUSSION

Gap Junctions are intercellular channels communicating the cytoplasmic space of adjacent cells. Each of the cells contributes with a hemichannel or connexon formed by a scaffold of six protein subunits, the connexins, that form a family of 21 members in humans [79]. They are selective channels that permit the pass of molecules up to 1 kDa in size, including all current-carrying anions and cations, glycolytic intermediates, vitamins, amino acids and nucleotides, as well as some of the more important second messengers involved in cell signaling, such as InsP3 and cAMP [91]. Gap junction channels are expressed in nearly all the tissues and systems of the organism [211] where the complexity of their function growths due to the intermixing of connexin subunits within the same channel. In the recent years it has been evident the importance of the normal function of these channels. Indeed, the aetiology of a great number of human hereditary diseases is related to mutations in the genes coding for connexins[69]. Currently, eight connexins have been firmly implicated in the pathogenesis of disorders of the peripheral nervous system (PNS) [212], skin[177], ear [213] and lens[69], as well as in a pleiotropic phenotype[214]. In some cases the pathogenic explanation seems to be straightforward due to the clear identification either on the loss-of-function mutations or large deletions which, by impairing intercellular communication, caused a specific deficit in cellular function[69,182]. However the explanation is not always so clear. Certain mutations have not been associated with an obvious functional deficit, and therefore, their pathogenic role has remained foggy.

## 4.1 Junctional-Conductance of Cx32 functional mutants involved in X-linked Charcot-Marie-Tooth disease

We have analysed the junctional coupling properties of a group of so-called functional mutations - i.e. R220stop, Δ11-116 and S26L - involved in CMTX [182,203,204,215,216].

The clinic consequences of Cx32 Δ11-116 and S26L mutations are obvious from our results showing an electrical blockade, indicating a drastic reduction in the channels cutoff. On the other hand, cells pairs transfected with Cx32 R220stop show a similar $G_j$ compared with the WT, consequently, it is possible that its pathologic effects are due to other subtle mechanisms. As the R220 residue is found at the C-terminus[217] the pathological relevance of this mutation could be related to the fast gating properties of the protein[110] as well as its ability in phosphorylation-dependent gating[218]. However these are questions to be resolved.

## 4.2 Junctional-Conductance analysis of molecular modified mutants causing genetic diseases

Lack of an atomic resolution structure of the gap junction has made it extremely difficult to conduct biochemical investigations within a consistent framework. We have analysed a group of mutations developed by the group of one of our collaborators, Dr. K. Avraham.

Based on a model of an intermediate resolution structure[205] they have developed second site mutagenesis to try to resolve some mechanistic processes due to pathology causing mutations.

From the results of our electrophysiological experiments done on these double mutated connexins (Cx26-S138N/N206S and R32E/E146R), it is clear that exists an exquisite wealth on details that determine the control of normal connexin function (see also[157]). They have focused on connexin localization; nevertheless the

fact to recover the normal localization in the contact membranes does not imply the functional recovery of the channel. As it is clear in figure 3-3, even though the doubly mutated channels recover a normal localization in the contact membranes, their conductance is absolutely absent. This shows that channels are not functional.

The same arguments can be stated in the case of the new isolated Cx26-L56V/M34T mutation. It was of interest to know if the L56V mutation was able, by itself, to induce deafness. Considering our results showing a $G_j$ comparable to the conductance of connexin WT and its pH-dependent gating, it is possible to conclude that it is only a polymorphism. The side chain steric properties of the Leucine and Valine do not seem to be so different to determine a drastic change in the characteristics of this protein. Moreover, our group has recently demonstrated that the Cx26-M34T mutation is related to impaired auditory function, forming channels that retain only 11% of the unitary conductance of the wild type channel. Most important, when co-expressed with HCx26wt at a 1:1 protein ratio, M34T invariably shows dominant-negative effects on cell–cell communication. These behaviors seem to be due to a constriction of the channel pore[210]. Considering that these two mutations are found in cis-conformation it could be possible that the L56V polimorphism is induced at a genetic level by the M34T mutation. Thus, we conclude that the pathologic consequences of the Cx26-L56V/M34T mutant have as origin the dominant effect of the M34T component.

As it is clear from these results, delicate interrelations between connexins and permeant molecules occur and consequently, changes in these interactions can result in channel malfunctioning. With this motivation we have also analysed the gap-junction unitary permeability to second messengers. We used novel ratiometric fluorescent biosensors that exploit the phenomenon of FRET for the quantitative monitoring of second messenger concentrations in real time. This approach may have a general impact as it permits to investigate the role second messengers in the physiology and pathology of cell-cell communication. The results and their discussion are described in the annexed article [95].

# REFERENCES


1. Pickles, J. O., Comis, S. D. & Osborne, M. P. Cross-links between stereocilia in the guinea pig organ of Corti, and their possible relation to sensory transduction. *Hear Res* **15**, 103-12 (1984).
2. Merchan, M. A., Merchan, J. A. & Ludena, M. D. Morphology of Hensen's cells. *J Anat* **131**, 519-23 (1980).
3. Spicer, S. S. & Schulte, B. A. Differences along the place-frequency map in the structure of supporting cells in the gerbil cochlea. *Hear Res* **79**, 161-77 (1994).
4. Yeaman, C., Grindstaff, K. K. & Nelson, W. J. New perspectives on mechanisms involved in generating epithelial cell polarity. *Physiol Rev* **79**, 73-98 (1999).
5. Wangemann, P., Schacht, J. in *The Cochlea* (ed. Dallos, P., Popper, A., Fay, R.) 130-185 (Springer-Verlag, New York, 1996).
6. von Bekesy, G. DC resting potential inside the cochlea partition. *J Acoust Soc Am* **24**, 72-76 (1952).
7. Marcus, D. *Acoustic Transduction* (ed. Sperelakis, N.) (Academic press, San Diego, California, USA, 1995).
8. Mammano, F. & Nobili, R. Biophysics of the cochlea: linear approximation. *J Acoust Soc Am* **93**, 3320-32 (1993).
9. Gillespie, P. G. & Walker, R. G. Molecular basis of mechanosensory transduction. *Nature* **413**, 194-202 (2001).
10. Corey, D. P. et al. TRPA1 is a candidate for the mechanosensitive transduction channel of vertebrate hair cells. *Nature* **432**, 723-730 (2004).
11. von Bekesy, G. Microphonics produced by touching the cochlear partition with a vibrating electrode. *J Acoust Soc Am* **23**, 29-35 (1951).
12. He, D. Z., Jia, S. & Dallos, P. Mechanoelectrical transduction of adult outer hair cells studied in a gerbil hemicochlea. *Nature* **429**, 766-70 (2004).
13. Cheatham, M. A. & Dallos, P. Longitudinal comparisons of IHC ac and dc receptor potentials recorded from the guinea pig cochlea. *Hear Res* **68**, 107-14 (1993).
14. Kennedy, H. J. & Meech, R. W. Fast Ca2+ signals at mouse inner hair cell synapse: a role for Ca2+-induced Ca2+ release. *J Physiol* **539**, 15-23 (2002).
15. Lelli, A. et al. Presynaptic calcium stores modulate afferent release in vestibular hair cells. *J Neurosci* **23**, 6894-903 (2003).
16. Lioudyno, M. et al. A "synaptoplasmic cistern" mediates rapid inhibition of cochlear hair cells. *J Neurosci* **24**, 11160-4 (2004).
17. Cousillas, H., Cole, K. S. & Johnstone, B. M. Effect of spider venom on cochlear nerve activity consistent with glutamatergic transmission at hair cell-afferent dendrite synapse. *Hear Res* **36**, 213-20 (1988).

18. Parsons, T. D., Lenzi, D., Almers, W. & Roberts, W. M. Calcium-triggered exocytosis and endocytosis in an isolated presynaptic cell: capacitance measurements in saccular hair cells. *Neuron* **13**, 875-83 (1994).
19. Beutner, D., Voets, T., Neher, E. & Moser, T. Calcium dependence of exocytosis and endocytosis at the cochlear inner hair cell afferent synapse. *Neuron* **29**, 681-90 (2001).
20. Fuchs, P. The synaptic physiology of cochlear hair cells. *Audiol Neurootol* **7**, 40-4 (2002).
21. Glowatzki, E. & Fuchs, P. A. Transmitter release at the hair cell ribbon synapse. *Nat Neurosci* **5**, 147-54 (2002).
22. Keen, E. C. & Hudspeth, A. J. Transfer characteristics of the hair cell's afferent synapse. *Proc Natl Acad Sci U S A* **103**, 5537-42 (2006).
23. Holt, J. C., Xue, J. T., Brichta, A. M. & Goldberg, J. M. Transmission between type II hair cells and bouton afferents in the turtle posterior crista. *J Neurophysiol* **95**, 428-52 (2006).
24. Dallos, P. & Fakler, B. Prestin, a new type of motor protein. *Nat Rev Mol Cell Biol* **3**, 104-11 (2002).
25. Davis, H. An active process in cochlear mechanics. *Hear Res* **9**, 79-90 (1983).
26. Liberman, M. C. et al. Prestin is required for electromotility of the outer hair cell and for the cochlear amplifier. *Nature* **419**, 300-4 (2002).
27. Nobili, R. & Mammano, F. Biophysics of the cochlea. II: Stationary nonlinear phenomenology. *J Acoust Soc Am* **99**, 2244-55 (1996).
28. Scherer, M. P. & Gummer, A. W. Impedance analysis of the organ of corti with magnetically actuated probes. *Biophys J* **87**, 1378-91 (2004).
29. Fridberger, A. et al. Organ of corti potentials and the motion of the basilar membrane. *J Neurosci* **24**, 10057-63 (2004).
30. Greenwood, D. D. A cochlear frequency-position function for several species--29 years later. *J Acoust Soc Am* **87**, 2592-605 (1990).
31. Sadanaga, M. & Morimitsu, T. Development of endocochlear potential and its negative component in mouse cochlea. *Hear Res* **89**, 155-61 (1995).
32. Xia, A., Kikuchi, T., Hozawa, K., Katori, Y. & Takasaka, T. Expression of connexin 26 and Na,K-ATPase in the developing mouse cochlear lateral wall: functional implications. *Brain Res* **846**, 106-11 (1999).
33. Johnstone, B. M. & Sellick, P. M. The peripheral auditory apparatus. *Q Rev Biophys* **5**, 1-57 (1972).
34. Johnstone, B. M., Johnstone, J. R. & Pugsley, I. D. Membrane resistance in endolymphatic walls of the first turn of the guinea-pig cochlea. *J Acoust Soc Am* **40**, 1398-404 (1966).
35. Kitajiri, S. et al. Compartmentalization established by claudin-11-based tight junctions in stria vascularis is required for hearing through generation of endocochlear potential. *J Cell Sci* **117**, 5087-96 (2004).
36. Gow, A. et al. Deafness in Claudin 11-null mice reveals the critical contribution of basal cell tight junctions to stria vascularis function. *J Neurosci* **24**, 7051-62 (2004).

37. Takeuchi, S., Ando, M. & Kakigi, A. Mechanism generating endocochlear potential: role played by intermediate cells in stria vascularis. *Biophys J* **79**, 2572-82 (2000).
38. Marcus, D. C., Wu, T., Wangemann, P. & Kofuji, P. KCNJ10 (Kir4.1) potassium channel knockout abolishes endocochlear potential. *Am J Physiol Cell Physiol* **282**, C403-7 (2002).
39. Wangemann, P. K+ cycling and the endocochlear potential. *Hear Res* **165**, 1-9 (2002).
40. Marcus, D. C. et al. Protein kinase C mediates P2U purinergic receptor inhibition of K+ channel in apical membrane of strial marginal cells. *Hear Res* **115**, 82-92 (1998).
41. Offner, F. F., Dallos, P. & Cheatham, M. A. Positive endocochlear potential: mechanism of production by marginal cells of stria vascularis. *Hear Res* **29**, 117-24 (1987).
42. Wangemann, P., Shen, Z. & Liu, J. K(+)-induced stimulation of K+ secretion involves activation of the IsK channel in vestibular dark cells. *Hear Res* **100**, 201-10 (1996).
43. Housley, G. D., Greenwood, D. & Ashmore, J. F. Localization of cholinergic and purinergic receptors on outer hair cells isolated from the guinea-pig cochlea. *Proc R Soc Lond B Biol Sci* **249**, 265-73 (1992).
44. McGuirt, J. P. & Schulte, B. A. Distribution of immunoreactive alpha- and beta-subunit isoforms of Na,K-ATPase in the gerbil inner ear. *J Histochem Cytochem* **42**, 843-53 (1994).
45. Rarey, K. E., Ross, M. D. & Smith, C. B. Distribution and significance of norepinephrine in the lateral cochlear wall of pigmented and albino rats. *Hear Res* **6**, 15-23 (1982).
46. Wangemann, P., Liu, J., Shimozono, M., Schimanski, S. & Scofield, M. A. K+ secretion in strial marginal cells is stimulated via beta 1-adrenergic receptors but not via beta 2-adrenergic or vasopressin receptors. *J Membr Biol* **175**, 191-202 (2000).
47. Ishii, K., Zhai, W. G. & Akita, M. Effect of a beta-stimulant on the inner ear stria vascularis. *Ann Otol Rhinol Laryngol* **109**, 628-33 (2000).
48. Kanoh, N. Effect of norepinephrine on ouabain-sensitive, K+-dependent p-nitrophenylphosphatase activity in strial marginal cells of the cochlea in normal and reserpinized guinea pigs. *Acta Otolaryngol* **118**, 817-20 (1998).
49. Kanoh, N. Effects of epinephrine on ouabain-sensitive, K(+) -dependent P-nitrophenylphosphatase activity in strial marginal cells of guinea pigs. *Ann Otol Rhinol Laryngol* **108**, 345-8 (1999).
50. Sunose, H., Liu, J. & Marcus, D. C. cAMP increases K+ secretion via activation of apical IsK/KvLQT1 channels in strial marginal cells. *Hear Res* **114**, 107-16 (1997).
51. Marcus, D. C. & Chiba, T. K+ and Na+ absorption by outer sulcus epithelial cells. *Hear Res* **134**, 48-56 (1999).

52. Ricci, A. J., Crawford, A. C. & Fettiplace, R. Tonotopic variation in the conductance of the hair cell mechanotransducer channel. *Neuron* **40**, 983-90 (2003).
53. Jentsch, T. J. Neuronal KCNQ potassium channels: physiology and role in disease. *Nat Rev Neurosci* **1**, 21-30 (2000).
54. Kubisch, C. et al. KCNQ4, a novel potassium channel expressed in sensory outer hair cells, is mutated in dominant deafness. *Cell* **96**, 437-46 (1999).
55. Kharkovets, T. et al. KCNQ4, a K+ channel mutated in a form of dominant deafness, is expressed in the inner ear and the central auditory pathway. *Proc Natl Acad Sci U S A* **97**, 4333-8 (2000).
56. Fechner, F. P., Burgess, B. J., Adams, J. C., Liberman, M. C. & Nadol, J. B., Jr. Dense innervation of Deiters' and Hensen's cells persists after chronic deefferentation of guinea pig cochleas. *J Comp Neurol* **400**, 299-309 (1998).
57. Oesterle, E. C. & Dallos, P. Intracellular recordings from supporting cells in the guinea pig cochlea: DC potentials. *J Neurophysiol* **64**, 617-36 (1990).
58. Karwoski, C. J., Lu, H. K. & Newman, E. A. Spatial buffering of light-evoked potassium increases by retinal Muller (glial) cells. *Science* **244**, 578-80 (1989).
59. Skatchkov, S. N., Krusek, J., Reichenbach, A. & Orkand, R. K. Potassium buffering by Muller cells isolated from the center and periphery of the frog retina. *Glia* **27**, 171-80 (1999).
60. Boettger, T. et al. Deafness and renal tubular acidosis in mice lacking the K-Cl co-transporter Kcc4. *Nature* **416**, 874-8 (2002).
61. Lauf, P. K. & Adragna, N. C. K-Cl cotransport: properties and molecular mechanism. *Cell Physiol Biochem* **10**, 341-54 (2000).
62. Forge, A. et al. Gap junctions and connexin expression in the inner ear. *Novartis Found Symp* **219**, 134-50; discussion 151-6 (1999).
63. Santos-Sacchi, J. Isolated supporting cells from the organ of Corti: some whole cell electrical characteristics and estimates of gap junctional conductance. *Hear Res* **52**, 89-98 (1991).
64. Forge, A. Gap junctions in the stria vascularis and effects of ethacrynic acid. *Hear Res* **13**, 189-200 (1984).
65. Mizuta, K., Adachi, M. & Iwasa, K. H. Ultrastructural localization of the Na-K-Cl cotransporter in the lateral wall of the rabbit cochlear duct. *Hear Res* **106**, 154-62 (1997).
66. Hibino, H. et al. Expression of an inwardly rectifying K+ channel, Kir5.1, in specific types of fibrocytes in the cochlear lateral wall suggests its functional importance in the establishment of endocochlear potential. *Eur J Neurosci* **19**, 76-84 (2004).
67. Kumar, N. M. & Gilula, N. B. The gap junction communication channel. *Cell* **84**, 381-8 (1996).
68. Harris, A. L. Emerging issues of connexin channels: biophysics fills the gap. *Q Rev Biophys* **34**, 325-472 (2001).
69. Gerido, D. A. & White, T. W. Connexin disorders of the ear, skin, and lens. *Biochim Biophys Acta* **1662**, 159-70 (2004).

70. Bruzzone, R., White, T. W. & Paul, D. L. Connections with connexins: the molecular basis of direct intercellular signaling. *Eur J Biochem* **238**, 1-27 (1996).
71. Unger, V. M., Kumar, N. M., Gilula, N. B. & Yeager, M. Projection structure of a gap junction membrane channel at 7 A resolution. *Nat Struct Biol* **4**, 39-43 (1997).
72. Unger, V. M., Kumar, N. M., Gilula, N. B. & Yeager, M. Three-dimensional structure of a recombinant gap junction membrane channel. *Science* **283**, 1176-80 (1999).
73. Foote, C. I., Zhou, L., Zhu, X. & Nicholson, B. J. The pattern of disulfide linkages in the extracellular loop regions of connexin 32 suggests a model for the docking interface of gap junctions. *J Cell Biol* **140**, 1187-97 (1998).
74. Purnick, P. E., Benjamin, D. C., Verselis, V. K., Bargiello, T. A. & Dowd, T. L. Structure of the amino terminus of a gap junction protein. *Arch Biochem Biophys* **381**, 181-90 (2000).
75. Purnick, P. E., Oh, S., Abrams, C. K., Verselis, V. K. & Bargiello, T. A. Reversal of the gating polarity of gap junctions by negative charge substitutions in the N-terminus of connexin 32. *Biophys J* **79**, 2403-15 (2000).
76. Arita, K. et al. A novel N14Y mutation in Connexin26 in keratitis-ichthyosis-deafness syndrome: analyses of altered gap junctional communication and molecular structure of N terminus of mutated Connexin26. *Am J Pathol* **169**, 416-23 (2006).
77. Duffy, H. S. et al. pH-dependent intramolecular binding and structure involving Cx43 cytoplasmic domains. *J Biol Chem* **277**, 36706-14 (2002).
78. Sorgen, P. L. et al. Sequence-specific resonance assignment of the carboxyl terminal domain of Connexin43. *J Biomol NMR* **23**, 245-6 (2002).
79. Willecke, K. et al. Structural and functional diversity of connexin genes in the mouse and human genome. *Biol Chem* **383**, 725-37 (2002).
80. Beyer, E. C. a. W., K. in *Gap Junction* (ed. E., B.) 1-29 (Hertzberg, 2000).
81. Laird, D. W. Life cycle of connexins in health and disease. *Biochem J* **394**, 527-43 (2006).
82. George, C. H., Kendall, J. M. & Evans, W. H. Intracellular trafficking pathways in the assembly of connexins into gap junctions. *J Biol Chem* **274**, 8678-85 (1999).
83. Kikuchi, T., Kimura, R. S., Paul, D. L. & Adams, J. C. Gap junctions in the rat cochlea: immunohistochemical and ultrastructural analysis. *Anat Embryol (Berl)* **191**, 101-18 (1995).
84. Sosinsky, G. Mixing of connexins in gap junction membrane channels. *Proc Natl Acad Sci U S A* **92**, 9210-4 (1995).
85. Gemel, J., Valiunas, V., Brink, P. R. & Beyer, E. C. Connexin43 and connexin26 form gap junctions, but not heteromeric channels in co-expressing cells. *J Cell Sci* **117**, 2469-80 (2004).

86. Segretain, D. & Falk, M. M. Regulation of connexin biosynthesis, assembly, gap junction formation, and removal. *Biochim Biophys Acta* **1662**, 3-21 (2004).
87. Sosinsky, G. E. et al. Tetracysteine genetic tags complexed with biarsenical ligands as a tool for investigating gap junction structure and dynamics. *Cell Commun Adhes* **10**, 181-6 (2003).
88. Lampe, P. D. & Lau, A. F. The effects of connexin phosphorylation on gap junctional communication. *Int J Biochem Cell Biol* **36**, 1171-86 (2004).
89. Lampe, P. D., Cooper, C. D., King, T. J. & Burt, J. M. Analysis of Connexin43 phosphorylated at S325, S328 and S330 in normoxic and ischemic heart. *J Cell Sci* **119**, 3435-42 (2006).
90. Lawrence, T. S., Beers, W. H. & Gilula, N. B. Transmission of hormonal stimulation by cell-to-cell communication. *Nature* **272**, 501-6 (1978).
91. Goldberg, G. S., Valiunas, V. & Brink, P. R. Selective permeability of gap junction channels. *Biochim Biophys Acta* **1662**, 96-101 (2004).
92. Suchyna, T. M. et al. Different ionic selectivities for connexins 26 and 32 produce rectifying gap junction channels. *Biophys J* **77**, 2968-87 (1999).
93. Veenstra, R. D. et al. Selectivity of connexin-specific gap junctions does not correlate with channel conductance. *Circ Res* **77**, 1156-65 (1995).
94. Elfgang, C. et al. Specific permeability and selective formation of gap junction channels in connexin-transfected HeLa cells. *J Cell Biol* **129**, 805-17 (1995).
95. Hernandez, V. H. et al. Unitary permeability of gap junction channels to second messengers measured by FRET microscopy. *Nat Methods* **4**, 353-8 (2007).
96. Bukauskas, F. F., Elfgang, C., Willecke, K. & Weingart, R. Heterotypic gap junction channels (connexin26-connexin32) violate the paradigm of unitary conductance. *Pflugers Arch* **429**, 870-2 (1995).
97. Bukauskas, F. F. & Verselis, V. K. Gap junction channel gating. *Biochim Biophys Acta* **1662**, 42-60 (2004).
98. Bennett, M. V. Gap junctions as electrical synapses. *J Neurocytol* **26**, 349-66 (1997).
99. Bukauskas, F. F. & Weingart, R. Multiple conductance states of newly formed single gap junction channels between insect cells. *Pflugers Arch* **423**, 152-4 (1993).
100. Verselis, V. K., Ginter, C. S. & Bargiello, T. A. Opposite voltage gating polarities of two closely related connexins. *Nature* **368**, 348-51 (1994).
101. Oh, S., Rubin, J. B., Bennett, M. V., Verselis, V. K. & Bargiello, T. A. Molecular determinants of electrical rectification of single channel conductance in gap junctions formed by connexins 26 and 32. *J Gen Physiol* **114**, 339-64 (1999).
102. Oh, S., Abrams, C. K., Verselis, V. K. & Bargiello, T. A. Stoichiometry of transjunctional voltage-gating polarity reversal by a negative charge substitution in the amino terminus of a connexin32 chimera. *J Gen Physiol* **116**, 13-31 (2000).

103. Oh, S., Rivkin, S., Tang, Q., Verselis, V. K. & Bargiello, T. A. Determinants of gating polarity of a connexin 32 hemichannel. *Biophys J* **87**, 912-28 (2004).
104. Rubin, J. B., Verselis, V. K., Bennett, M. V. & Bargiello, T. A. Molecular analysis of voltage dependence of heterotypic gap junctions formed by connexins 26 and 32. *Biophys J* **62**, 183-93; discussion 193-5 (1992).
105. Rubin, J. B., Verselis, V. K., Bennett, M. V. & Bargiello, T. A. A domain substitution procedure and its use to analyze voltage dependence of homotypic gap junctions formed by connexins 26 and 32. *Proc Natl Acad Sci U S A* **89**, 3820-4 (1992).
106. Revilla, A., Castro, C. & Barrio, L. C. Molecular dissection of transjunctional voltage dependence in the connexin-32 and connexin-43 junctions. *Biophys J* **77**, 1374-83 (1999).
107. Gonzalez, D., Gomez-Hernandez, J. M. & Barrio, L. C. Molecular basis of voltage dependence of connexin channels: an integrative appraisal. *Prog Biophys Mol Biol* **94**, 66-106 (2007).
108. Peracchia, C., Salim, M. & Peracchia, L. L. Unusual slow gating of gap junction channels in oocytes expressing connexin32 or its COOH-terminus truncated mutant. *J Membr Biol* **215**, 161-8 (2007).
109. Barrio, L. C., Capel, J., Jarillo, J. A., Castro, C. & Revilla, A. Species-specific voltage-gating properties of connexin-45 junctions expressed in Xenopus oocytes. *Biophys J* **73**, 757-69 (1997).
110. Revilla, A., Bennett, M. V. & Barrio, L. C. Molecular determinants of membrane potential dependence in vertebrate gap junction channels. *Proc Natl Acad Sci U S A* **97**, 14760-5 (2000).
111. Cottrell, G. T., Lin, R., Warn-Cramer, B. J., Lau, A. F. & Burt, J. M. Mechanism of v-Src- and mitogen-activated protein kinase-induced reduction of gap junction communication. *Am J Physiol Cell Physiol* **284**, C511-20 (2003).
112. Duncan, J. C. & Fletcher, W. H. alpha 1 Connexin (connexin43) gap junctions and activities of cAMP-dependent protein kinase and protein kinase C in developing mouse heart. *Dev Dyn* **223**, 96-107 (2002).
113. Shi, X. et al. A novel casein kinase 2 alpha-subunit regulates membrane protein traffic in the human hepatoma cell line HuH-7. *J Biol Chem* **276**, 2075-82 (2001).
114. John, S., Cesario, D. & Weiss, J. N. Gap junctional hemichannels in the heart. *Acta Physiol Scand* **179**, 23-31 (2003).
115. Takens-Kwak, B. R. & Jongsma, H. J. Cardiac gap junctions: three distinct single channel conductances and their modulation by phosphorylating treatments. *Pflugers Arch* **422**, 198-200 (1992).
116. Saez, J. C. et al. cAMP increases junctional conductance and stimulates phosphorylation of the 27-kDa principal gap junction polypeptide. *Proc Natl Acad Sci U S A* **83**, 2473-7 (1986).
117. Saez, J. C. et al. Phosphorylation of connexin 32, a hepatocyte gap-junction protein, by cAMP-dependent protein kinase, protein kinase C and

Ca2+/calmodulin-dependent protein kinase II. *Eur J Biochem* **192**, 263-73 (1990).
118. Chanson, M., White, M. M. & Garber, S. S. cAMP promotes gap junctional coupling in T84 cells. *Am J Physiol* **271**, C533-9 (1996).
119. Traub, O. et al. Comparative characterization of the 21-kD and 26-kD gap junction proteins in murine liver and cultured hepatocytes. *J Cell Biol* **108**, 1039-51 (1989).
120. Kwak, B. R. et al. Differential regulation of distinct types of gap junction channels by similar phosphorylating conditions. *Mol Biol Cell* **6**, 1707-19 (1995).
121. Locke, D., Koreen, I. V. & Harris, A. L. Isoelectric points and post-translational modifications of connexin26 and connexin32. *Faseb J* **20**, 1221-3 (2006).
122. Peracchia, C. Chemical gating of gap junction channels; roles of calcium, pH and calmodulin. *Biochim Biophys Acta* **1662**, 61-80 (2004).
123. Peracchia, C., Wang, X. G. & Peracchia, L. L. Chemical gating of gap junction channels. *Methods* **20**, 188-95 (2000).
124. Peracchia, C., Sotkis, A., Wang, X. G., Peracchia, L. L. & Persechini, A. Calmodulin directly gates gap junction channels. *J Biol Chem* **275**, 26220-4 (2000).
125. Burr, G. S., Mitchell, C. K., Keflemariam, Y. J., Heidelberger, R. & O'Brien, J. Calcium-dependent binding of calmodulin to neuronal gap junction proteins. *Biochem Biophys Res Commun* **335**, 1191-8 (2005).
126. Zhou, Y. et al. Identification of the calmodulin binding domain of connexin 43. *J Biol Chem* **282**, 35005-17 (2007).
127. Stergiopoulos, K. et al. Hetero-domain interactions as a mechanism for the regulation of connexin channels. *Circ Res* **84**, 1144-55 (1999).
128. Young, K. C. & Peracchia, C. Opposite Cx32 and Cx26 voltage-gating response to CO2 reflects opposite voltage-gating polarity. *J Membr Biol* **202**, 161-70 (2004).
129. Peracchia, C., Wang, X., Li, L. & Peracchia, L. L. Inhibition of calmodulin expression prevents low-pH-induced gap junction uncoupling in Xenopus oocytes. *Pflugers Arch* **431**, 379-87 (1996).
130. White, R. L., Doeller, J. E., Verselis, V. K. & Wittenberg, B. A. Gap junctional conductance between pairs of ventricular myocytes is modulated synergistically by H+ and Ca++. *J Gen Physiol* **95**, 1061-75 (1990).
131. Forge, A. & Wright, T. The molecular architecture of the inner ear. *Br Med Bull* **63**, 5-24 (2002).
132. Kikuchi, T., Adams, J. C., Paul, D. L. & Kimura, R. S. Gap junction systems in the rat vestibular labyrinth: immunohistochemical and ultrastructural analysis. *Acta Otolaryngol* **114**, 520-8 (1994).
133. Jagger, D. J. & Forge, A. Compartmentalized and signal-selective gap junctional coupling in the hearing cochlea. *J Neurosci* **26**, 1260-8 (2006).

134. Yum, S. W. et al. Human connexin26 and connexin30 form functional heteromeric and heterotypic channels. *Am J Physiol Cell Physiol* **293**, C1032-48 (2007).
135. Dahl, E. et al. Molecular cloning and functional expression of mouse connexin-30,a gap junction gene highly expressed in adult brain and skin. *J Biol Chem* **271**, 17903-10 (1996).
136. Kelley, P. M. et al. Human connexin 30 (GJB6), a candidate gene for nonsyndromic hearing loss: molecular cloning, tissue-specific expression, and assignment to chromosome 13q12. *Genomics* **62**, 172-6 (1999).
137. Buniello, A., Montanaro, D., Volinia, S., Gasparini, P. & Marigo, V. An expression atlas of connexin genes in the mouse. *Genomics* **83**, 812-20 (2004).
138. Cohen-Salmon, M. et al. Expression of the connexin43- and connexin45-encoding genes in the developing and mature mouse inner ear. *Cell Tissue Res* **316**, 15-22 (2004).
139. Morton, C. C. Gene discovery in the auditory system using a tissue specific approach. *Am J Med Genet A* **130**, 26-8 (2004).
140. Carrasquillo, M. M., Zlotogora, J., Barges, S. & Chakravarti, A. Two different connexin 26 mutations in an inbred kindred segregating non-syndromic recessive deafness: implications for genetic studies in isolated populations. *Hum Mol Genet* **6**, 2163-72 (1997).
141. Denoyelle, F. et al. Prelingual deafness: high prevalence of a 30delG mutation in the connexin 26 gene. *Hum Mol Genet* **6**, 2173-7 (1997).
142. Zelante, L. et al. Connexin26 mutations associated with the most common form of non-syndromic neurosensory autosomal recessive deafness (DFNB1) in Mediterraneans. *Hum Mol Genet* **6**, 1605-9 (1997).
143. Richard, G. Connexin gene pathology. *Clin Exp Dermatol* **28**, 397-409 (2003).
144. Chaib, H. et al. A gene responsible for a dominant form of neurosensory non-syndromic deafness maps to the NSRD1 recessive deafness gene interval. *Hum Mol Genet* **3**, 2219-22 (1994).
145. Stojkovic, T., Latour, P., Vandenberghe, A., Hurtevent, J. F. & Vermersch, P. Sensorineural deafness in X-linked Charcot-Marie-Tooth disease with connexin 32 mutation (R142Q). *Neurology* **52**, 1010-4 (1999).
146. Liu, X. Z. et al. Mutations in connexin31 underlie recessive as well as dominant non-syndromic hearing loss. *Hum Mol Genet* **9**, 63-7 (2000).
147. Richard, G. et al. Mutations in the human connexin gene GJB3 cause erythrokeratodermia variabilis. *Nat Genet* **20**, 366-9 (1998).
148. Liu, X. Z. et al. Mutations in GJA1 (connexin 43) are associated with non-syndromic autosomal recessive deafness. *Hum Mol Genet* **10**, 2945-51 (2001).
149. Xia, J. H. et al. Mutations in the gene encoding gap junction protein beta-3 associated with autosomal dominant hearing impairment. *Nat Genet* **20**, 370-3 (1998).
150. Grifa, A. et al. Mutations in GJB6 cause nonsyndromic autosomal dominant deafness at DFNA3 locus. *Nat Genet* **23**, 16-8 (1999).

151. Kelsell, D. P. et al. Connexin 26 mutations in hereditary non-syndromic sensorineural deafness. *Nature* **387**, 80-3 (1997).
152. White, T. W., Deans, M. R., Kelsell, D. P. & Paul, D. L. Connexin mutations in deafness. *Nature* **394**, 630-1 (1998).
153. Estivill, X. et al. Connexin-26 mutations in sporadic and inherited sensorineural deafness. *Lancet* **351**, 394-8 (1998).
154. Van Laer, L. et al. A common founder for the 35delG GJB2 gene mutation in connexin 26 hearing impairment. *J Med Genet* **38**, 515-8 (2001).
155. Morell, R. J. et al. Mutations in the connexin 26 gene (GJB2) among Ashkenazi Jews with nonsyndromic recessive deafness. *N Engl J Med* **339**, 1500-5 (1998).
156. Bruzzone, R. et al. Functional analysis of a dominant mutation of human connexin26 associated with nonsyndromic deafness. *Cell Commun Adhes* **8**, 425-31 (2001).
157. Beltramello, M., Piazza, V., Bukauskas, F. F., Pozzan, T. & Mammano, F. Impaired permeability to Ins(1,4,5)P(3) in a mutant connexin underlies recessive hereditary deafness. *Nat Cell Biol* **7**, 63-9 (2005).
158. Denoyelle, F. et al. Connexin 26 gene linked to a dominant deafness. *Nature* **393**, 319-20 (1998).
159. Loffler, J. et al. Sensorineural hearing loss and the incidence of Cx26 mutations in Austria. *Eur J Hum Genet* **9**, 226-30 (2001).
160. Morle, L. et al. A novel C202F mutation in the connexin26 gene (GJB2) associated with autosomal dominant isolated hearing loss. *J Med Genet* **37**, 368-70 (2000).
161. Piazza, V. et al. Functional analysis of R75Q mutation in the gene coding for Connexin 26 identified in a family with nonsyndromic hearing loss. *Clin Genet* **68**, 161-6 (2005).
162. Common, J. E. et al. Functional studies of human skin disease- and deafness-associated connexin 30 mutations. *Biochem Biophys Res Commun* **298**, 651-6 (2002).
163. del Castillo, I. et al. A deletion involving the connexin 30 gene in nonsyndromic hearing impairment. *N Engl J Med* **346**, 243-9 (2002).
164. Del Castillo, I. et al. Prevalence and evolutionary origins of the del(GJB6-D13S1830) mutation in the DFNB1 locus in hearing-impaired subjects: a multicenter study. *Am J Hum Genet* **73**, 1452-8 (2003).
165. Lopez-Bigas, N. et al. Connexin 31 (GJB3) is expressed in the peripheral and auditory nerves and causes neuropathy and hearing impairment. *Hum Mol Genet* **10**, 947-52 (2001).
166. Di, W. L. et al. Defective trafficking and cell death is characteristic of skin disease-associated connexin 31 mutations. *Hum Mol Genet* **11**, 2005-14 (2002).
167. White, T. W. & Paul, D. L. Genetic diseases and gene knockouts reveal diverse connexin functions. *Annu Rev Physiol* **61**, 283-310 (1999).

168. Gabriel, H. D. et al. Transplacental uptake of glucose is decreased in embryonic lethal connexin26-deficient mice. *J Cell Biol* **140**, 1453-61 (1998).
169. Cohen-Salmon, M. et al. Targeted ablation of connexin26 in the inner ear epithelial gap junction network causes hearing impairment and cell death. *Curr Biol* **12**, 1106-11 (2002).
170. Lautermann, J. et al. Expression of the gap-junction connexins 26 and 30 in the rat cochlea. *Cell Tissue Res* **294**, 415-20 (1998).
171. Valiunas, V., Manthey, D., Vogel, R., Willecke, K. & Weingart, R. Biophysical properties of mouse connexin30 gap junction channels studied in transfected human HeLa cells. *J Physiol* **519 Pt 3**, 631-44 (1999).
172. Teubner, B. et al. Connexin30 (Gjb6)-deficiency causes severe hearing impairment and lack of endocochlear potential. *Hum Mol Genet* **12**, 13-21 (2003).
173. Cohen-Salmon, M. et al. Connexin30 deficiency causes instrastrial fluid-blood barrier disruption within the cochlear stria vascularis. *Proc Natl Acad Sci U S A* **104**, 6229-34 (2007).
174. Ahmad, S. et al. Restoration of connexin26 protein level in the cochlea completely rescues hearing in a mouse model of human connexin30-linked deafness. *Proc Natl Acad Sci U S A* **104**, 1337-41 (2007).
175. Brissette, J. L., Kumar, N. M., Gilula, N. B., Hall, J. E. & Dotto, G. P. Switch in gap junction protein expression is associated with selective changes in junctional permeability during keratinocyte differentiation. *Proc Natl Acad Sci U S A* **91**, 6453-7 (1994).
176. Kelsell, D. P., Di, W. L. & Houseman, M. J. Connexin mutations in skin disease and hearing loss. *Am J Hum Genet* **68**, 559-68 (2001).
177. Richard, G. Connexin disorders of the skin. *Adv Dermatol* **17**, 243-77 (2001).
178. Lamartine, J. et al. Mutations in GJB6 cause hidrotic ectodermal dysplasia. *Nat Genet* **26**, 142-4 (2000).
179. Birouk, N. et al. X-linked Charcot-Marie-Tooth disease with connexin 32 mutations: clinical and electrophysiologic study. *Neurology* **50**, 1074-82 (1998).
180. Anzini, P. et al. Structural abnormalities and deficient maintenance of peripheral nerve myelin in mice lacking the gap junction protein connexin 32. *J Neurosci* **17**, 4545-51 (1997).
181. Bergoffen, J. et al. Connexin mutations in X-linked Charcot-Marie-Tooth disease. *Science* **262**, 2039-42 (1993).
182. Oh, S. et al. Changes in permeability caused by connexin 32 mutations underlie X-linked Charcot-Marie-Tooth disease. *Neuron* **19**, 927-38 (1997).
183. Balice-Gordon, R. J., Bone, L. J. & Scherer, S. S. Functional gap junctions in the schwann cell myelin sheath. *J Cell Biol* **142**, 1095-104 (1998).
184. Llopis, J., McCaffery, J. M., Miyawaki, A., Farquhar, M. G. & Tsien, R. Y. Measurement of cytosolic, mitochondrial, and Golgi pH in single living cells with green fluorescent proteins. *Proc Natl Acad Sci U S A* **95**, 6803-8 (1998).

185. Matsuyama, S., Llopis, J., Deveraux, Q. L., Tsien, R. Y. & Reed, J. C. Changes in intramitochondrial and cytosolic pH: early events that modulate caspase activation during apoptosis. *Nat Cell Biol* **2**, 318-25 (2000).
186. Thompson, R. B., Whetsell, W. O., Jr., Maliwal, B. P., Fierke, C. A. & Frederickson, C. J. Fluorescence microscopy of stimulated Zn(II) release from organotypic cultures of mammalian hippocampus using a carbonic anhydrase-based biosensor system. *J Neurosci Methods* **96**, 35-45 (2000).
187. Jayaraman, S., Haggie, P., Wachter, R. M., Remington, S. J. & Verkman, A. S. Mechanism and cellular applications of a green fluorescent protein-based halide sensor. *J Biol Chem* **275**, 6047-50 (2000).
188. Baird, G. S., Zacharias, D. A. & Tsien, R. Y. Circular permutation and receptor insertion within green fluorescent proteins. *Proc Natl Acad Sci U S A* **96**, 11241-6 (1999).
189. Miyawaki, A. et al. Fluorescent indicators for Ca2+ based on green fluorescent proteins and calmodulin. *Nature* **388**, 882-7 (1997).
190. Miyawaki, A., Griesbeck, O., Heim, R. & Tsien, R. Y. Dynamic and quantitative Ca2+ measurements using improved cameleons. *Proc Natl Acad Sci U S A* **96**, 2135-40 (1999).
191. Nakai, J., Ohkura, M. & Imoto, K. A high signal-to-noise Ca(2+) probe composed of a single green fluorescent protein. *Nat Biotechnol* **19**, 137-41 (2001).
192. Wouters, F. S., Verveer, P. J. & Bastiaens, P. I. Imaging biochemistry inside cells. *Trends Cell Biol* **11**, 203-11 (2001).
193. Gu, Y., Di, W. L., Kelsell, D. P. & Zicha, D. Quantitative fluorescence resonance energy transfer (FRET) measurement with acceptor photobleaching and spectral unmixing. *J Microsc* **215**, 162-73 (2004).
194. Wlodarczyk, J. et al. Analysis of FRET-signals in the presence of free donors and acceptors. *Biophys J* (2007).
195. Ponsioen, B. et al. Detecting cAMP-induced Epac activation by fluorescence resonance energy transfer: Epac as a novel cAMP indicator. *EMBO Rep* **5**, 1176-80 (2004).
196. Qu, Y. & Dahl, G. Function of the voltage gate of gap junction channels: selective exclusion of molecules. *Proc Natl Acad Sci U S A* **99**, 697-702 (2002).
197. Bedner, P. et al. Selective permeability of different connexin channels to the second messenger cyclic AMP. *J Biol Chem* **281**, 6673-81 (2006).
198. Saez, J. C., Connor, J. A., Spray, D. C. & Bennett, M. V. Hepatocyte gap junctions are permeable to the second messenger, inositol 1,4,5-trisphosphate, and to calcium ions. *Proc Natl Acad Sci U S A* **86**, 2708-12 (1989).
199. Tanimura, A., Nezu, A., Morita, T., Turner, R. J. & Tojyo, Y. Fluorescent biosensor for quantitative real-time measurements of inositol 1,4,5-trisphosphate in single living cells. *J Biol Chem* **279**, 38095-8 (2004).
200. Mammano, F. et al. An optical recording system based on a fast CCD sensor for biological imaging. *Cell Calcium* **25**, 115-23 (1999).

201. Bastianello S., C. C. D., Beltramello M., Mammano F. in *Proceedings of SPIE* 265-274 (2004).
202. Downes, C. P., Mussat, M. C. & Michell, R. H. The inositol trisphosphate phosphomonoesterase of the human erythrocyte membrane. *Biochem J* **203**, 169-77 (1982).
203. Ressot, C., Gomes, D., Dautigny, A., Pham-Dinh, D. & Bruzzone, R. Connexin32 mutations associated with X-linked Charcot-Marie-Tooth disease show two distinct behaviors: loss of function and altered gating properties. *J Neurosci* **18**, 4063-75 (1998).
204. Wang, H. L. et al. Functional analysis of connexin-32 mutants associated with X-linked dominant Charcot-Marie-Tooth disease. *Neurobiol Dis* **15**, 361-70 (2004).
205. Fleishman, S. J., Unger, V. M., Yeager, M. & Ben-Tal, N. A Calpha model for the transmembrane alpha helices of gap junction intercellular channels. *Mol Cell* **15**, 879-88 (2004).
206. Evans, W. H. & Martin, P. E. Gap junctions: structure and function (Review). *Mol Membr Biol* **19**, 121-36 (2002).
207. Fleishman, S. J., Sabag, A. D., Ophir, E., Avraham, K. B. & Ben-Tal, N. The structural context of disease-causing mutations in gap junctions. *J Biol Chem* **281**, 28958-63 (2006).
208. Kenna, M. A., Wu, B. L., Cotanche, D. A., Korf, B. R. & Rehm, H. L. Connexin 26 studies in patients with sensorineural hearing loss. *Arch Otolaryngol Head Neck Surg* **127**, 1037-42 (2001).
209. Marlin, S. et al. Connexin 26 gene mutations in congenitally deaf children: pitfalls for genetic counseling. *Arch Otolaryngol Head Neck Surg* **127**, 927-33 (2001).
210. Bicego, M. et al. Pathogenetic role of the deafness-related M34T mutation of Cx26. *Hum Mol Genet* **15**, 2569-87 (2006).
211. Saez, J. C., Berthoud, V. M., Branes, M. C., Martinez, A. D. & Beyer, E. C. Plasma membrane channels formed by connexins: their regulation and functions. *Physiol Rev* **83**, 1359-400 (2003).
212. Bone, L. J., Deschenes, S. M., Balice-Gordon, R. J., Fischbeck, K. H. & Scherer, S. S. Connexin32 and X-linked Charcot-Marie-Tooth disease. *Neurobiol Dis* **4**, 221-30 (1997).
213. Petit, C., Levilliers, J. & Hardelin, J. P. Molecular genetics of hearing loss. *Annu Rev Genet* **35**, 589-646 (2001).
214. Paznekas, W. A. et al. Connexin 43 (GJA1) mutations cause the pleiotropic phenotype of oculodentodigital dysplasia. *Am J Hum Genet* **72**, 408-18 (2003).
215. Abrams, C. K., Freidin, M. M., Verselis, V. K., Bennett, M. V. & Bargiello, T. A. Functional alterations in gap junction channels formed by mutant forms of connexin 32: evidence for loss of function as a pathogenic mechanism in the X-linked form of Charcot-Marie-Tooth disease. *Brain Res* **900**, 9-25 (2001).
216. Abrams, C. K., Bennett, M. V., Verselis, V. K. & Bargiello, T. A. Voltage opens unopposed gap junction hemichannels formed by a connexin 32 mutant

associated with X-linked Charcot-Marie-Tooth disease. *Proc Natl Acad Sci U S A* **99**, 3980-4 (2002).
217. Bicego, M. et al. Selective defects in channel permeability associated with Cx32 mutations causing X-linked Charcot-Marie-Tooth disease. *Neurobiol Dis* **21**, 607-17 (2006).
218. Zhou, L., Kasperek, E. M. & Nicholson, B. J. Dissection of the molecular basis of pp60(v-src) induced gating of connexin 43 gap junction channels. *J Cell Biol* **144**, 1033-45 (1999).